Dark Matter and Lepton Flavour Violation in Seesaw Models

Jorge C. Romão
Instituto Superior Técnico, Departamento de Física & CFTP
A. Rovisco Pais 1, 1049-001 Lisboa, Portugal

November 18^{th}, 2010

Summary

- Motivation
- The Setup
- Results
- Conclusions

Collaborators: J. N. Esteves, M. Hirsch, W. Porod, S. Kaneko, A. Villanova del Moral, F. Staub

Articles: arXiv:0903.1408 [JHEP05(2009)003], arXiv:0907.5090 [PRD80(2009)095003] & arXiv:1010.6000

Dark Matter

- Standard cosmology requires the existence of a non-baryonic dark matter (DM) contribution to the total energy budget of the universe.
- In the past few years estimates of the DM abundance have become increasingly precise. The Particle Data Group now quotes at 1 σ c.l.

$$\Omega_{DM} h^2 = 0.110 \pm 0.006$$

- Since the data from the WMAP satellite and large scale structure formation is best fitted if the DM is cold, weakly interacting mass particles (WIMP) are currently the preferred explanation. While there is certainly no shortage of WIMP candidates, the literature is completely dominated by studies of the lightest neutralino.

In 1980 Weinberg noticed that the dimension-five operator

$$\mathcal{L}_{\text{Dim5}} = L H_u \, L H_u$$

could induce neutrino masses:

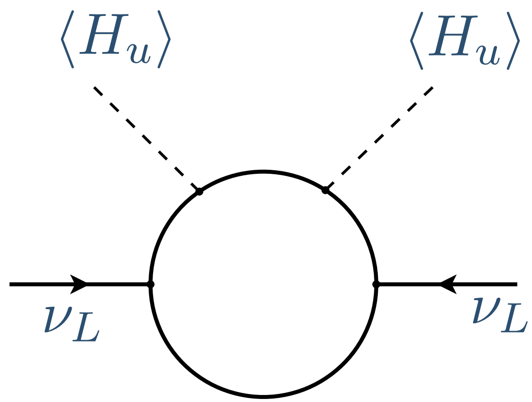

S. Weinberg, Phys. Rev. D **22**, 1694 (1980)

Type I mechanism

In models with singlet RH neutrinos

$$\mathcal{L} = H_u \, \overline{\nu_L} \, Y_\nu \, \nu_R - \frac{1}{2} \nu_R^T \, C^{-1} \, M_R \, \nu_R$$

we obtain

$$m_{\text{eff}}^{\text{I}} = -(vY_\nu) M_R^{-1} (vY_\nu)^T$$

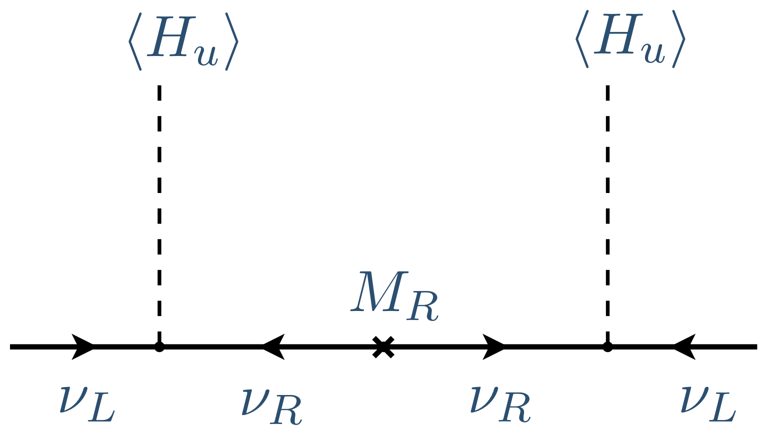

Minkowski, Gell-Mann, Ramond, Slansky, Yanagida, Mohapatra, Senjanovic

Type II mechanism

In models with scalar Higgs Triplets

$$-\mathcal{L} = \frac{1}{2} Y_\Delta \overline{\nu_L^c} i\tau_2 \Delta_L \nu_L + \mu H_u^T \Delta_L H_u + M_\Delta^2 \Delta_L^\dagger \Delta_L + \cdots$$

we obtain

$$m_{\text{eff}}^{\text{II}} = \frac{v^2 \mu Y_\Delta}{M_\Delta^2}$$

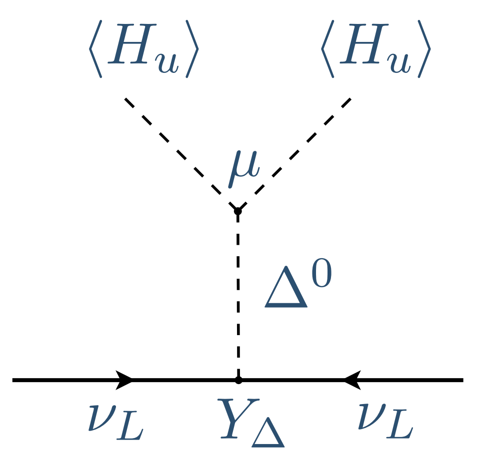

Schechter, Valle, Mohapatra, Senjanovic, Lazarides, Shafi, Wetterich

Type III mechanism

In models with triplet fermions

$$\mathcal{L} = H_u \overline{W_M} Y_\nu^{\mathrm{III}} \nu_L - \frac{1}{2} W_M^T C^{-1} M_{W_M} W_M$$

we obtain

$$m_{\mathrm{eff}}^{\mathrm{III}} = -(v Y_\nu^{\mathrm{III}}) M_{W_M}^{-1} (v Y_\nu^{\mathrm{III}})^T$$

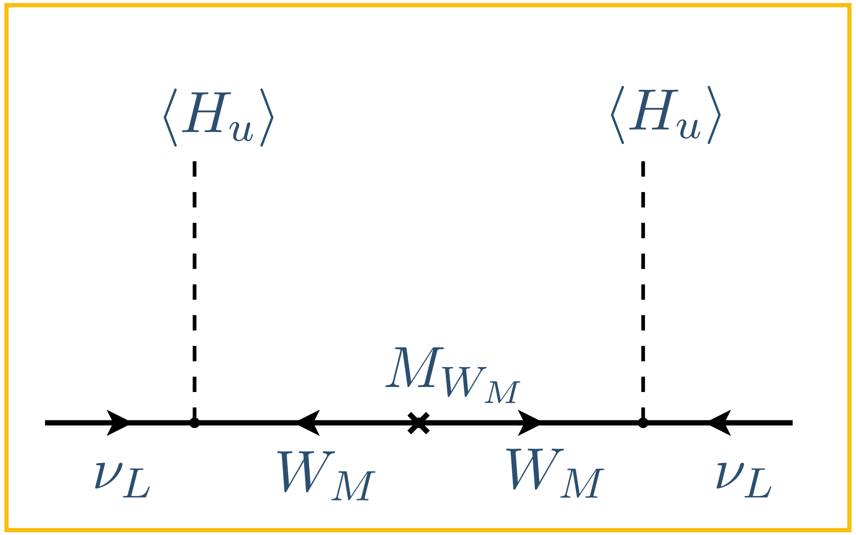

Minkowski, Gell-Mann, Ramond, Slansky, Yanagida, Mohapatra, Senjanovic

Neutralino Dark Matter

In mSugra only four very specific regions can explain the WMAP data:

- The bulk region
- The co-annihilation line
- The "focus point" line
- The "higgs funnel" region (large $\tan\beta$)

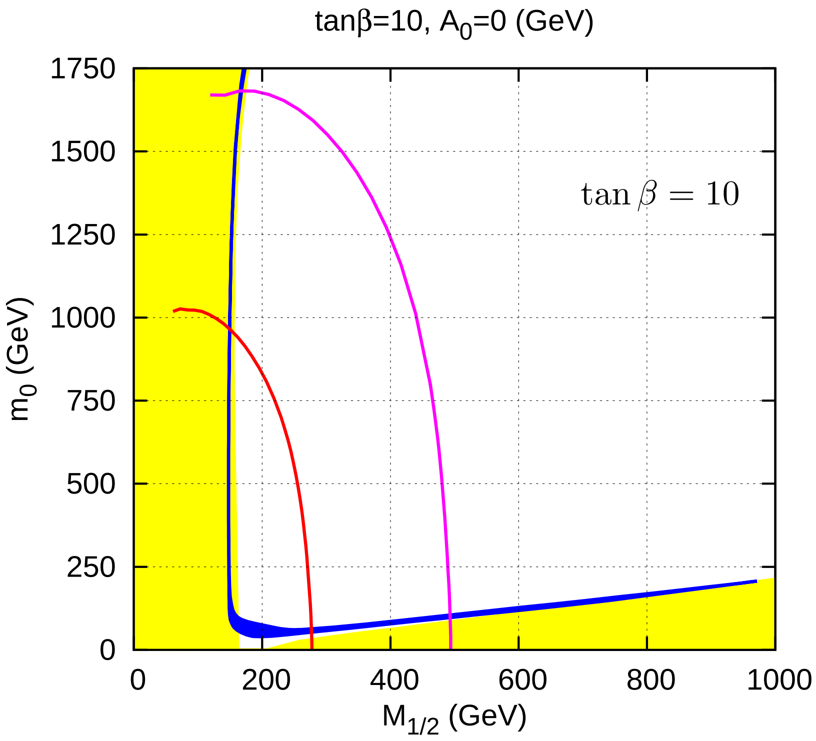

We will consider neutralino dark matter within a supersymmetric type-I, type-II and type-III seesaw models with mSugra boundary conditions. For type-II and III, the deformed sparticle spectrum with respect to mSugra expectations leads to characteristic changes in the allowed regions as a function of the unknown seesaw scale.

Running of the soft parameters

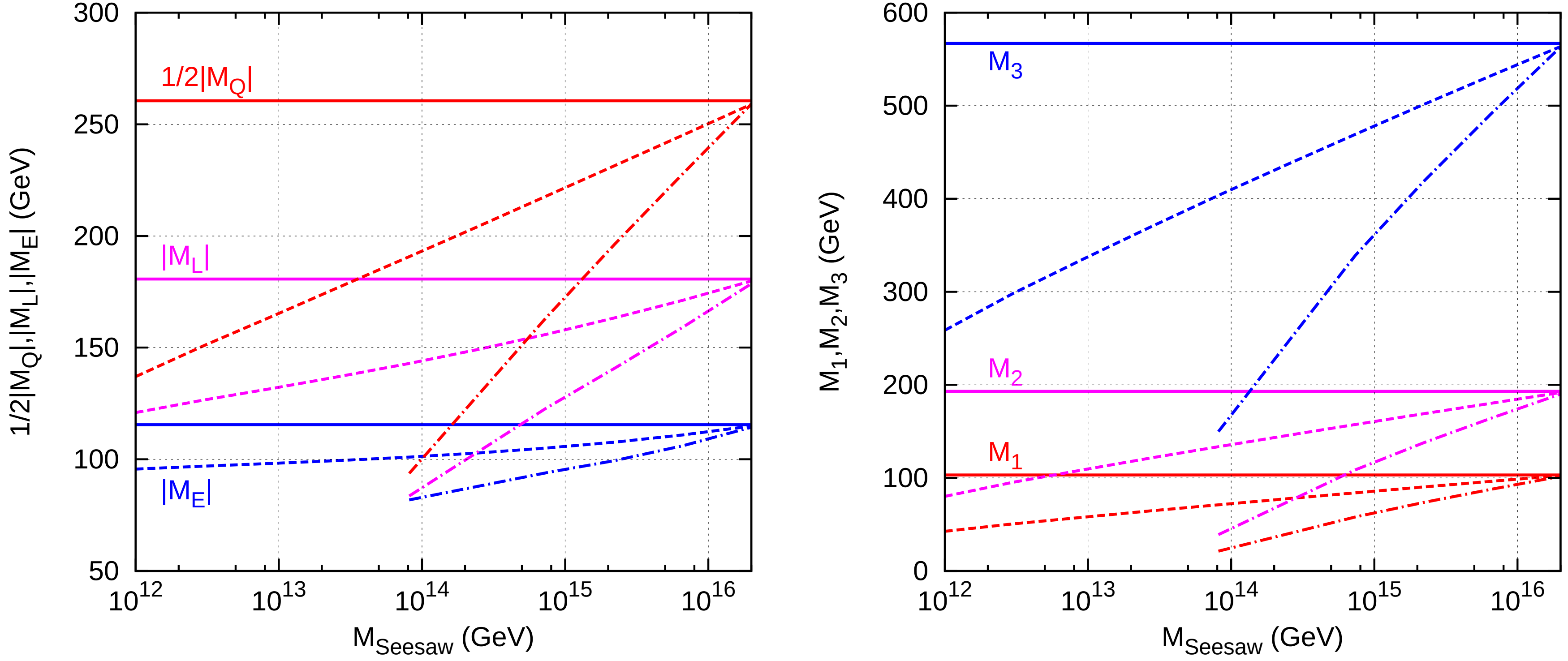

Numerically calculated running of scalar (to the left) and gaugino mass parameters (to the right), at two-loop level. The mass parameters are calculated as a function of M_{Seesaw} for the mSugra parameters $m_0 = 70$ GeV and $M_{1/2} = 250$ GeV for seesaw type-I (solid line), type-II (dashed line) and type-III (dot-dashed line). For $M_{\text{Seesaw}} \simeq 2 \times 10^{16}$ GeV the mSugra values are recovered. Smaller M_{Seesaw} lead to smaller soft masses in all cases. Note that the running is different for the different mass parameters with gaugino masses running faster than slepton mass parameters.

Being complex symmetric, the light Majorana neutrino mass matrix is diagonalized by a unitary 3×3 matrix U

$$\hat{m}_\nu = U^T \cdot m_\nu \cdot U$$

For U we will use the standard form

$$U = \begin{pmatrix} c_{12}c_{13} & s_{12}c_{13} & s_{13}e^{-i\delta} \\ -s_{12}c_{23} - c_{12}s_{23}s_{13}e^{i\delta} & c_{12}c_{23} - s_{12}s_{23}s_{13}e^{i\delta} & s_{23}c_{13} \\ s_{12}s_{23} - c_{12}c_{23}s_{13}e^{i\delta} & -c_{12}s_{23} - s_{12}c_{23}s_{13}e^{i\delta} & c_{23}c_{13} \end{pmatrix} \times \begin{pmatrix} e^{i\alpha_1/2} & 0 & 0 \\ 0 & e^{i\alpha_2/2} & 0 \\ 0 & 0 & 1 \end{pmatrix}$$

parameter	best fit	2-σ
$\Delta m^2_{21}[10^{-5}\text{eV}^2]$	$7.59^{+0.23}_{-0.18}$	$7.22 - 8.03$
$\lvert\Delta m^2_{31}\rvert[10^{-3}\text{eV}^2]$	$2.40^{+0.12}_{-0.11}$	$2.18 - 2.64$
$\sin^2\theta_{12}$	$0.318^{+0.019}_{-0.016}$	$0.29 - 0.36$
$\sin^2\theta_{23}$	$0.50^{+0.07}_{-0.06}$	$0.39 - 0.63$
$\sin^2\theta_{13}$	$0.013^{+0.013}_{-0.009}$	≤ 0.039

$$U_{TBM} = \begin{pmatrix} \sqrt{\frac{2}{3}} & \sqrt{\frac{1}{3}} & 0 \\ -\frac{1}{\sqrt{6}} & \frac{1}{\sqrt{3}} & -\frac{1}{\sqrt{2}} \\ -\frac{1}{\sqrt{6}} & \frac{1}{\sqrt{3}} & \frac{1}{\sqrt{2}} \end{pmatrix}$$

Lepton Flavour Violation (LFV)

All these seesaw models have built in LFV, as they are models for neutrino masses. LFV is highly constrained . We summarize the current bounds on the LFV observables, as well as the future sensitivity.

LFV process	Present bound	Future sensitivity
BR($\mu \to e\gamma$)	1.2×10^{-11}	10^{-13}
BR($\tau \to e\gamma$)	1.1×10^{-7}	10^{-9}
BR($\tau \to \mu\gamma$)	4.5×10^{-8}	10^{-9}
BR($\mu \to 3e$)	1.0×10^{-12}	
BR($\tau \to 3e$)	3.6×10^{-8}	2×10^{-10}
BR($\tau \to 3\mu$)	3.2×10^{-8}	2×10^{-10}
CR($\mu - e$, Ti)	4.3×10^{-12}	$\mathcal{O}(10^{-16})$ ($\mathcal{O}(10^{-18})$)
CR($\mu - e$, Au)	7×10^{-13}	
CR($\mu - e$, Al)		$\mathcal{O}(10^{-16})$

The Setup: GUT scale

At GUT scale the SU(5) invariant superpotentials are

- Type-I

$$W_{\rm RHN} = \mathbf{Y}_N^{\rm I}\ N^c\ \bar{5}\cdot 5_H + \frac{1}{2}\ M_R\ N^c N^c$$

- Type-II

$$\begin{aligned} W_{\rm 15H} =& \frac{1}{\sqrt{2}}\mathbf{Y}_N^{\rm II}\ \bar{5}\cdot 15\cdot\bar{5} + \frac{1}{\sqrt{2}}\lambda_1\bar{5}_H\cdot 15\cdot\bar{5}_H + \frac{1}{\sqrt{2}}\lambda_2 5_H\cdot\overline{15}\cdot 5_H \\ &+\mathbf{Y}_5 10\cdot\bar{5}\cdot\bar{5}_H + \mathbf{Y}_{10}10\cdot 10\cdot 5_H + M_{15}15\cdot\overline{15} + M_5\bar{5}_H\cdot 5_H \end{aligned}$$

- Type-III

$$\begin{aligned} W_{\rm 24H} =& \sqrt{2}\,\bar{5}_M Y^5 10_M \bar{5}_H - \frac{1}{4}10_M Y^{10} 10_M 5_H + 5_H 24_M Y_N^{III}\bar{5}_M \\ &+\frac{1}{2}24_M M_{24} 24_M \end{aligned}$$

The $SU(5)$-broken phase

Under $SU(3) \times SU_L(2) \times U(1)_Y$

- The $\mathbf{5}$, $\mathbf{10}$ and $\mathbf{5}_H$ contain

$$\bar{5} = (d^c, L), \;\; 10 = (u^c, e^c, Q), \;\; 5_H = (H^c, H_u), \;\; \bar{5}_H = (\bar{H}^c, H_d)$$

- The $\mathbf{15}$ decomposes as

$$\mathbf{15} = S(6, 1, -\frac{2}{3}) + T(1, 3, 1) + Z(3, 2, \frac{1}{6})$$

- The $\mathbf{24}$ decomposes as

$$\mathbf{24} = W_M(1, 3, 0) + B_M(1, 1, 0) + \overline{X}_M(3, 2, -\frac{5}{6}) + X_M(\bar{3}, 2, \frac{5}{6}) + G_M(8, 1, 0)$$

Supersymmetric seesaw type-I

In the case of seesaw type-I one postulates very heavy right-handed neutrinos yielding the following superpotential below M_{GUT}:

$$\begin{aligned} W_I =& W_{MSSM} + W_\nu \ , \\ W_\nu =& \widehat{N}^c Y_\nu \widehat{L} \cdot \widehat{H}_u + \frac{1}{2} \widehat{N}^c M_R \widehat{N}^c \ , \end{aligned}$$

For the neutrino mass matrix one obtains the well-known formula

$$m_\nu = -\frac{v_u^2}{2} Y_\nu^T M_R^{-1} Y_\nu$$

Inverting the seesaw equation, allows to express Y_ν as (Casas & Ibarra)

$$Y_\nu = \sqrt{2}\frac{i}{v_u}\sqrt{\hat{M}_R} \cdot R \cdot \sqrt{\hat{m}_\nu} \cdot U^\dagger$$

where the $\hat{m}_\nu$ and $\hat{M}_R$ are diagonal matrices containing the corresponding eigenvalues. R is in general a complex orthogonal matrix.

Supersymmetric seesaw type-II

Below M_{GUT} in the $SU(5)$-broken phase the superpotential reads

$$\begin{aligned} W_{II} &= W_{MSSM} + \frac{1}{\sqrt{2}}(Y_T \widehat{L}\widehat{T}_1\widehat{L} + Y_S \widehat{D}^c \widehat{S}_1 \widehat{D}^c) + Y_Z \widehat{D}^c \widehat{Z}_1 \widehat{L} \\ &+ \frac{1}{\sqrt{2}}(\lambda_1 \widehat{H}_d \widehat{T}_1 \widehat{H}_d + \lambda_2 \widehat{H}_u \widehat{T}_2 \widehat{H}_u) + M_T \widehat{T}_1 \widehat{T}_2 + M_Z \widehat{Z}_1 \widehat{Z}_2 + M_S \widehat{S}_1 \widehat{S}_2 \end{aligned}$$

where fields with index 1 (2) originate from the 15-plet ($\overline{15}$-plet). The effective mass matrix is

$$m_\nu = -\frac{v_u^2}{2}\frac{\lambda_2}{M_T} Y_T.$$

Note that

$$\hat{Y}_T = U^T \cdot Y_T \cdot U \ ,$$

i.e. Y_T is diagonalized by the same matrix as m_ν. If all neutrino eigenvalues, angles and phases were known, Y_T would be fixed up to an overall constant.

In the $SU(5)$ broken phase the superpotential becomes

$$\begin{aligned} W_{III} \quad = \quad & W_{MSSM} + \widehat{H}_u(\widehat{W}_M Y_N - \sqrt{\frac{3}{10}}\widehat{B}_M Y_B)\widehat{L} + \widehat{H}_u \widehat{\bar{X}}_M Y_X \widehat{D}^c \\ & + \frac{1}{2}\widehat{B}_M M_B \widehat{B}_M + \frac{1}{2}\widehat{G}_M M_G \widehat{G}_M + \frac{1}{2}\widehat{W}_M M_W \widehat{W}_M + \widehat{X}_M M_X \widehat{\bar{X}}_M \end{aligned}$$

giving

$$m_\nu = -\frac{v_u^2}{2}\left(\frac{3}{10} Y_B^T M_B^{-1} Y_B + \frac{1}{2} Y_W^T M_W^{-1} Y_W\right) \simeq -v_u^2 \frac{4}{10} Y_W^T M_W^{-1} Y_W$$

where the last step is justified as we start from universal couplings and masses at M_{GUT} we find that at the seesaw scale one still has $M_B \simeq M_W$ and $Y_B \simeq Y_W$. One can use the corresponding Casas-Ibarra decomposition for Y_W as in type-I up to the overall factor $4/5$.

Effects of the heavy particles on the MSSM spectrum

The appearance of charged particles at scales between the electro-weak scale and the GUT scale leads to changes in the beta functions of the gauge couplings.

- In the MSSM the corresponding values at 1-loop level are $(b_1, b_2, b_3) = (33/5, 1, -3)$.
- In case of one **15**-plet the additional contribution is $\Delta b_i = 7/2$ whereas in case of **24**-plet it is $\Delta b_i = 5$. This results in case of type-II in a total shift of $\Delta b_i = 7$ for the minimal model and in case of type-III in $\Delta b_i = 15$ assuming 3 generations of **24**-plets.
- This does not only change the evolution of the gauge couplings but also the evolution of the gaugino and scalar mass parameters with profound implications on the spectrum. Additional effects on the spectrum of the scalars can be present if some of the Yukawa couplings get large.

Variation of the soft masses.

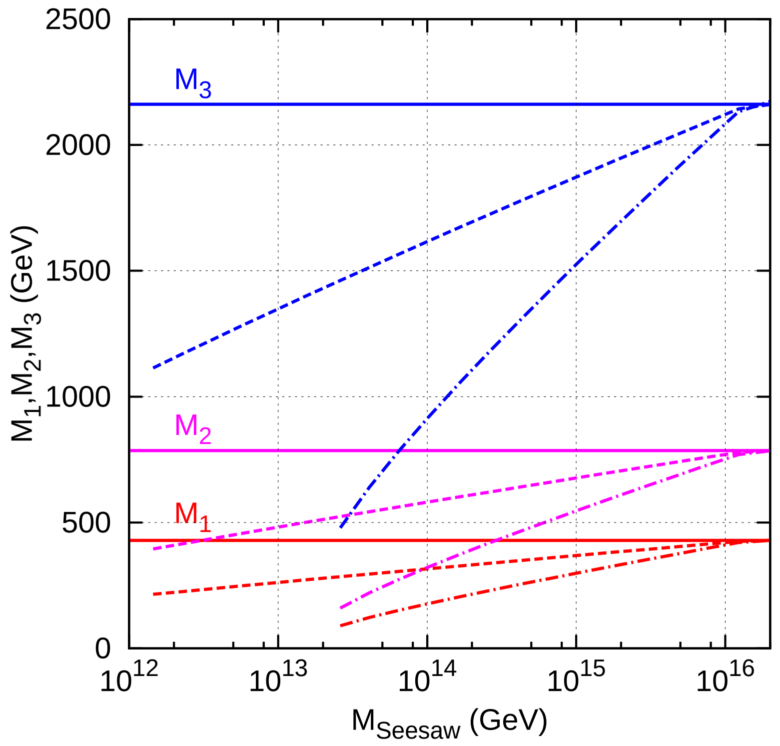

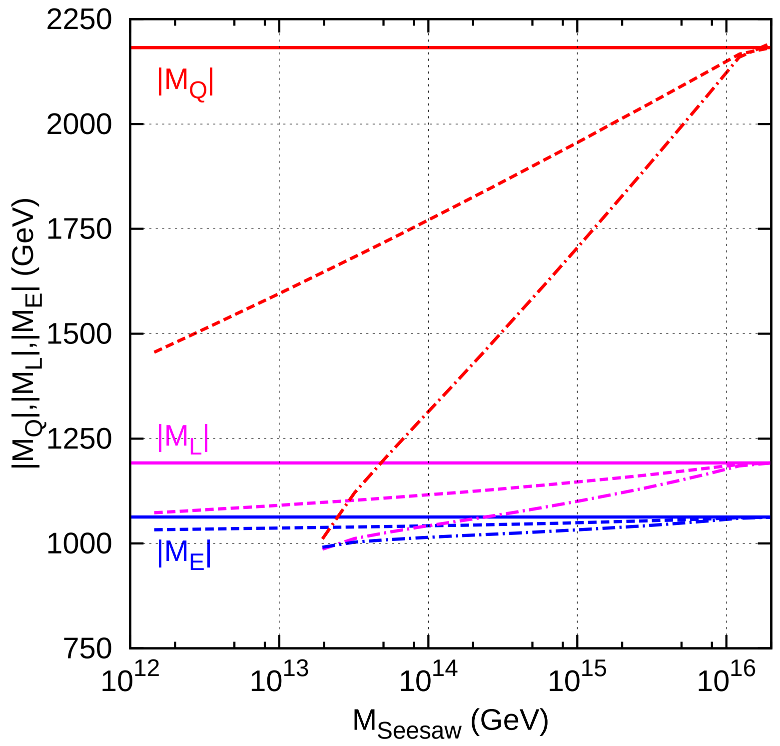

Mass parameters at $Q = 1$ TeV versus the seesaw scale for fixed high scale parameters $m_0 = M_{1/2} = 1$ TeV, $A_0 = 0$, $\tan\beta = 10$ and $\mu > 0$. The full lines correspond to seesaw type-I, the dashed ones to type-II and the dash-dotted ones to type-III. In all cases a degenerate spectrum of the seesaw particles has been assumed.

Variation on the Spectra

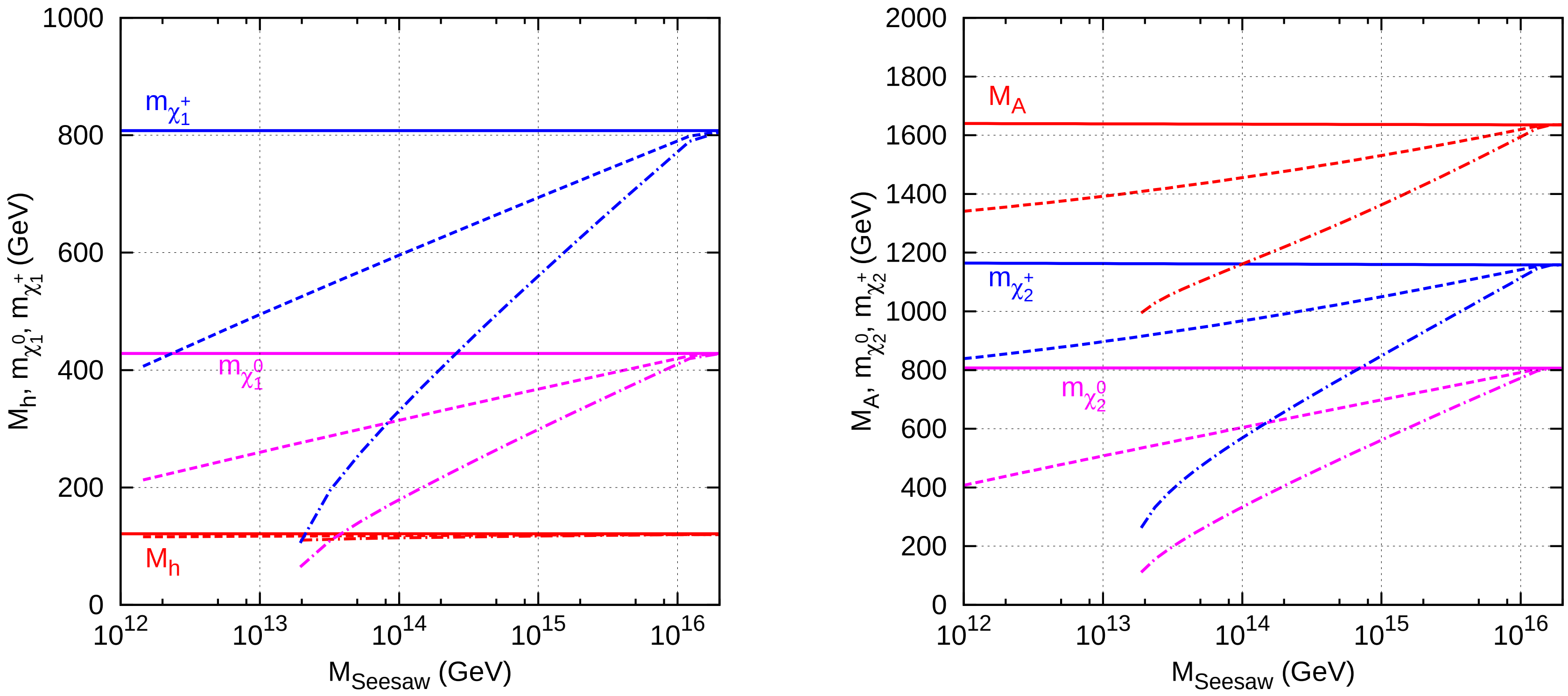

Example of spectra at $Q = 1$ TeV versus the seesaw scale for fixed high scale parameters $m_0 = M_{1/2} = 1$ TeV, $\tan\beta = 10$ and $\mu > 0$. On left panel $M_h, m_{\tilde{\chi}_1^0}, m_{\tilde{\chi}_1^+}$ while on the right panel we have $M_A, m_{\chi_2^0}, m_{\tilde{\chi}_2^+}$.

Comparison for SPS3 ($M_{\text{Seesaw}} = 10^{14}$ GeV)

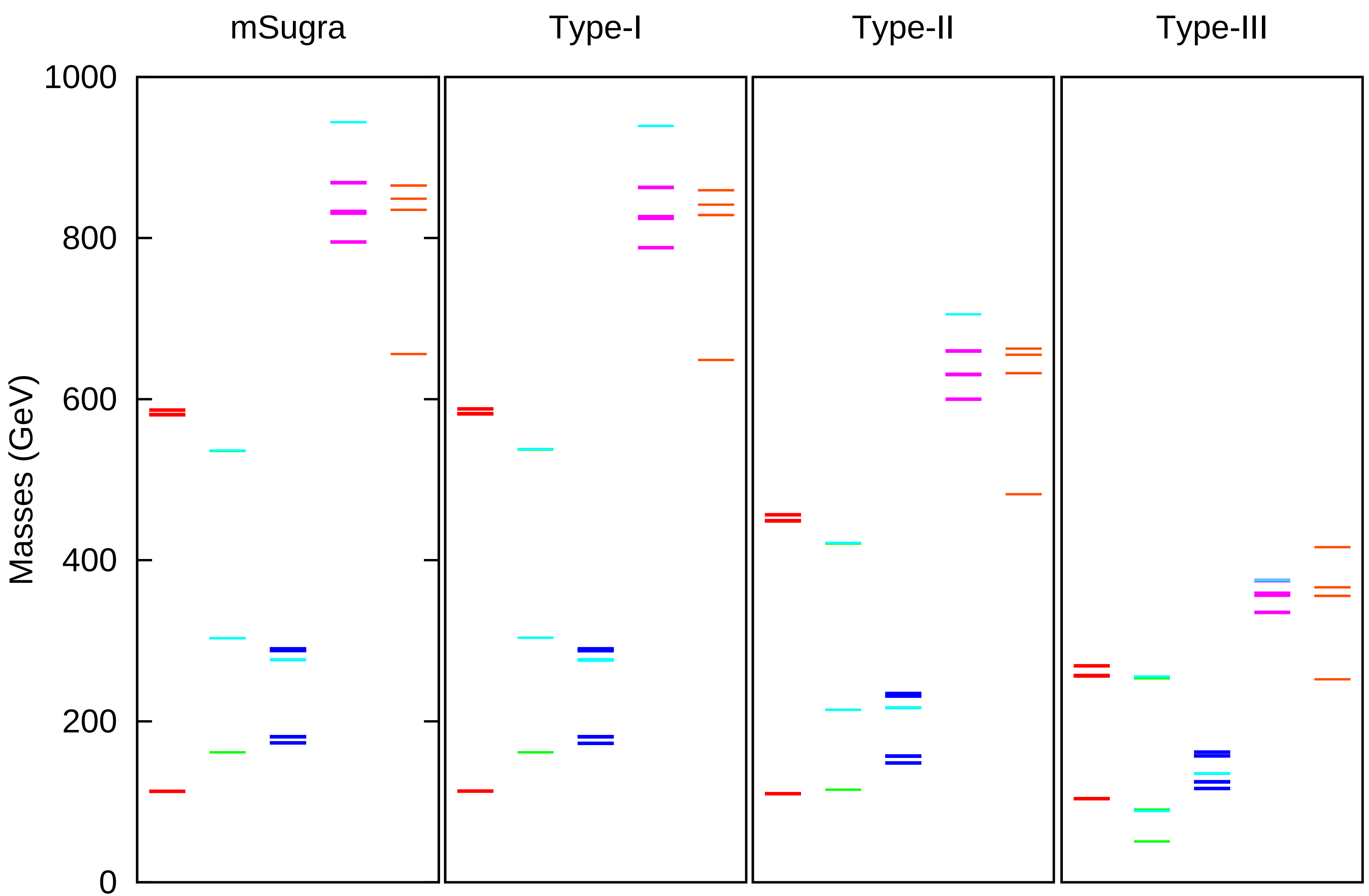

$m_0 = 90$ GeV, $M_{1/2} = 400$ GeV, $\tan\beta = 10$, $A_0 = 0$ GeV, $\mu > 0$

Invariant Combinations

- We note that in all three model types the ratio of the gaugino mass parameters is nearly the same as in the usual mSUGRA scenarios but the ratios of the sfermion mass parameters change.
- One can form four 'invariants' for which at least at the 1-loop level the dependence on $M_{1/2}$ and m_0 is rather weak

$$\frac{(m_L^2 - m_E^2)}{M_1^2}, \quad \frac{(m_Q^2 - m_E^2)}{M_1^2}, \quad \frac{(m_D^2 - m_L^2)}{M_1^2} \quad \text{and} \quad \frac{(m_Q^2 - m_U^2)}{M_1^2}.$$

- One concludes that in principle one has a handle to obtain information on the seesaw scale for given assumptions on the underlying neutrino mass model, if universal boundary conditions are assumed.

Invariant Combinations

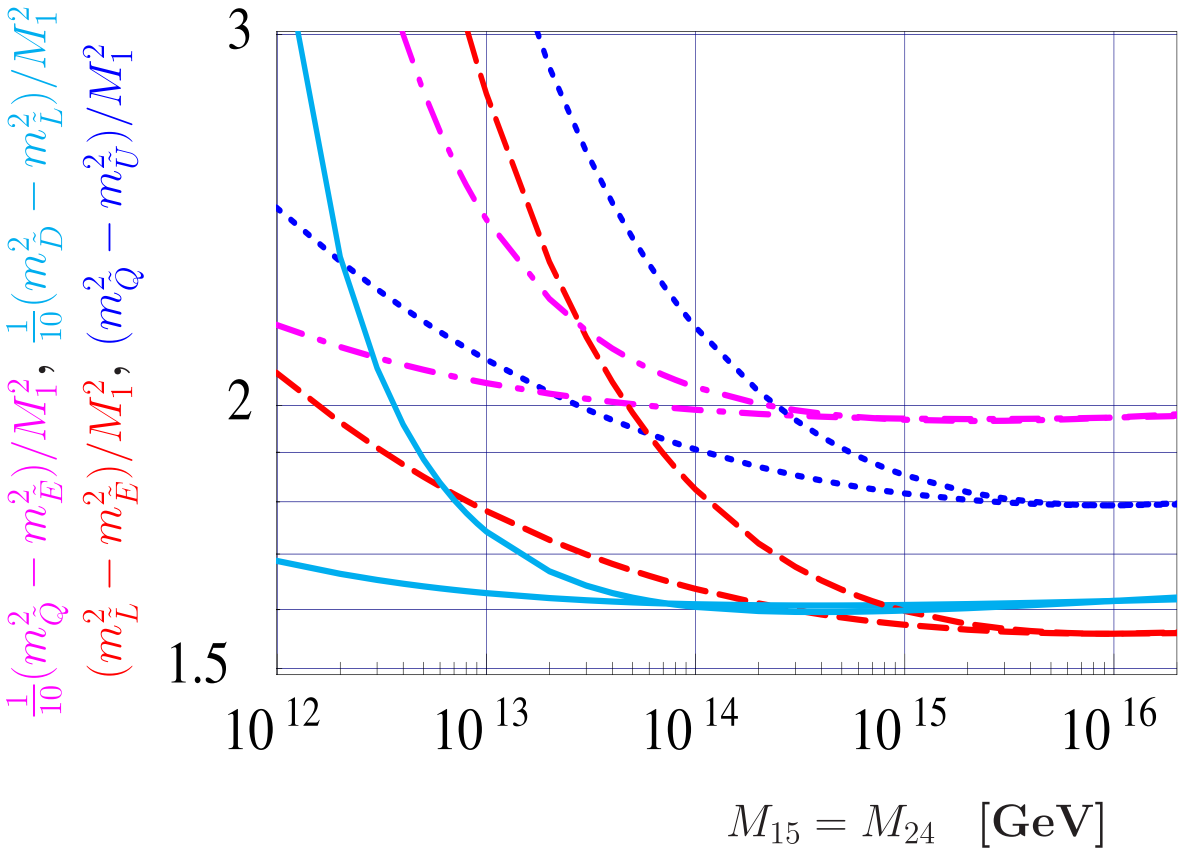

Four different "invariant" combinations of soft masses versus the mass of the **15**-plet *or* **24**-plet, $M_{15} = M_{24}$. The plot assumes that the Yukawa couplings are negligibly small. The calculation is at 1-loop order in the leading-log approximation. The lines running faster up towards smaller M are for type-III seesaw, the values for type-II seesaw are shown for comparison.

Invariant Combinations

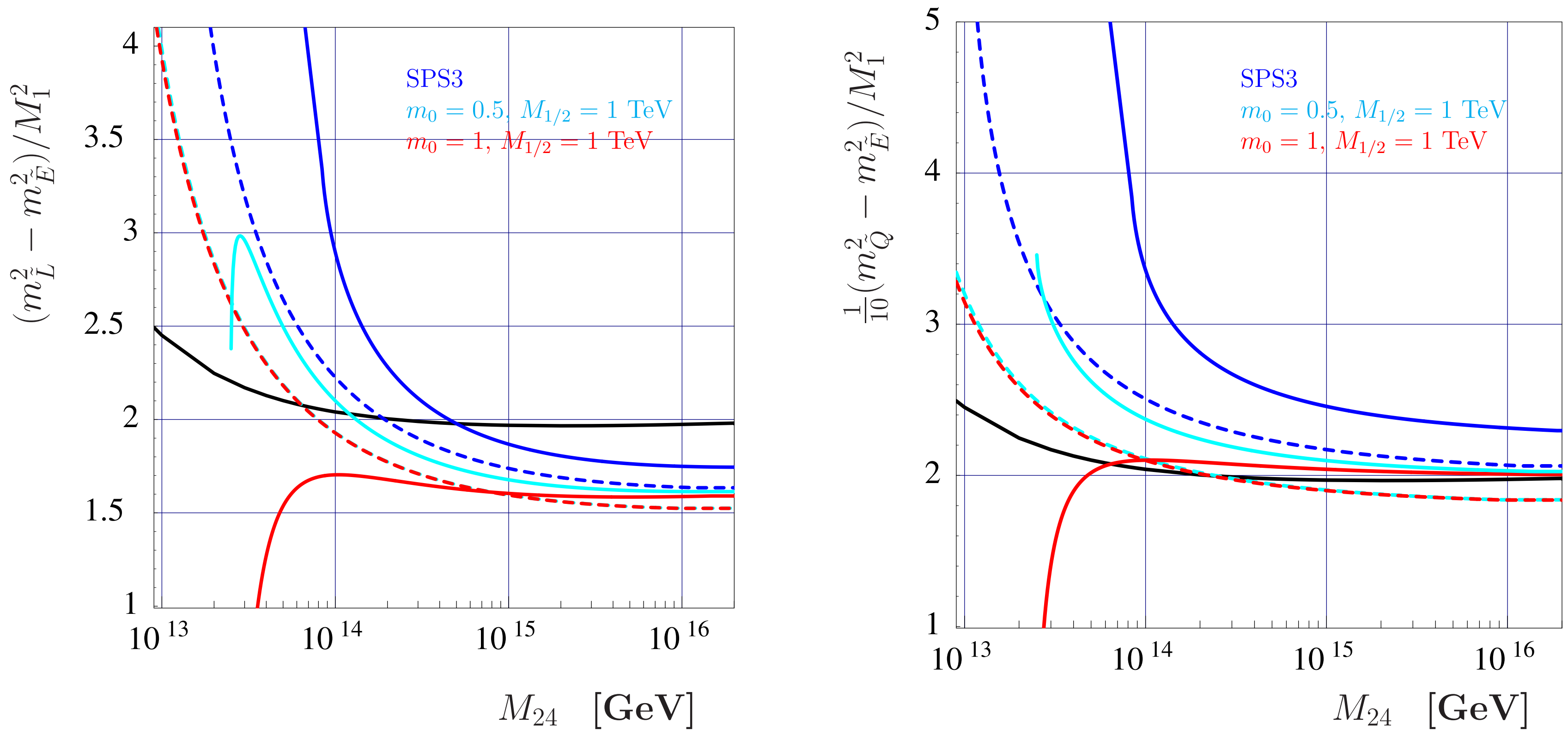

The limits of the invariants in seesaw type-III models. Left: $(m_L^2 - m_E^2)/M_1^2$, right $(m_Q^2 - m_E^2)/M_1^2$. The blue lines are for SPS3, the light blue one for $m_0 = 500$ GeV and $M_{1/2} = 1$ TeV, and the red one for $m_0 = M_{1/2} = 1$ TeV; full (dashed) lines are 2-loop (1-loop) results. The black line is the analytical approximation, for comparison.

Shift on M_{GUT}

- The use of the 2-loop RGEs leads to a shift of M_{GUT} from about 2×10^{16} GeV for **24**-plet mass of 10^{16} GeV to about 4×10^{16} GeV for **24**-plet mass of 10^{13} GeV, which is part of the differences between 1-loop and 2-loop.
- Here M_{GUT} is defined as the scale where the electro-weak couplings meet, e.g. $g_{U(1)} = g_{SU(2)}$. This implies also that there is some difference for the strong coupling which is, however, in the order of 5-10% which can easily be accounted for by threshold effects of the new GUT particles, e.g. the missing members of the gauge fields and the Higgs fields responsible for the breaking of the GUT group.
- A second reason why the deviations between the leading log calculation, the case of 1-loop and 2-loop RGEs gets larger for smaller seesaw scale is that the increase of the beta coefficients implies larger values of the gauge couplings at the GUT scale. This implies that one reaches a Landau pole for sufficiently low values of the seesaw scale.
- In the numerical calculation we find very often that one of the scalar masses squared, in particular staus and/or sbottoms, gets large negative values already for values of the seesaw scale larger than the Landau pole.

Landau Poles

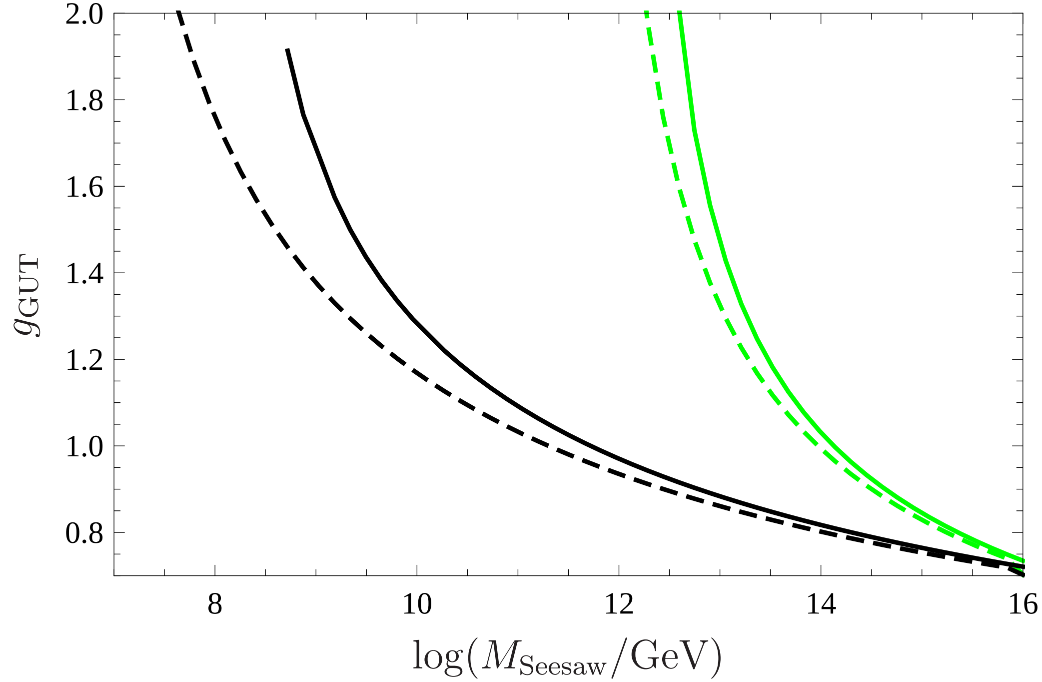

Values of the gauge coupling at $M_{GUT} = 2 \times 10^{16}$ GeV as a function of the seesaw scale, black lines seesaw type-II and green lines seesaw type-III with three **24**-plets with degenerate mass spectrum; full (dashed) lines are 2-loop (1-loop) results. For the calculation of the electroweak threshold the spectrum corresponds to $m_0 = M_{1/2} = 1$ TeV, $A_0 = 0$, $\tan\beta = 10$ and $\mu > 0$.

LFV in the slepton sector: Approximate formulas

From a one-step integration of the RGEs one gets assuming mSUGRA boundary conditions a first rough estimate for the lepton flavour violating entries in the slepton mass parameters

$$m^2_{L,ij} \simeq -\frac{a_k}{8\pi^2}\left(3m_0^2 + A_0^2\right)\left(Y_N^{k,\dagger} L Y_N^k\right)_{ij}$$

$$A_{l,ij} \simeq -a_k \frac{3}{16\pi^2} A_0 \left(Y_e Y_N^{k,\dagger} L Y_N^k\right)_{ij}$$

for $i \neq j$ in the basis where Y_e is diagonal, $L_{ij} = \ln(M_{GUT}/M_i)\delta_{ij}$ and Y_N^k is the additional Yukawa coupling of the type-k seesaw at M_{GUT} and

$$a_I = 1\ ,\ a_{II} = 6 \text{ and } a_{III} = \frac{9}{5}$$

LFV in the slepton sector: Approximate formulas

- All models have in common that they predict negligible flavour violation for the right-sleptons

$$m^2_{E,ij} \simeq 0$$

- We know that these approximations work well only in case of the type-I models. Nevertheless they give a rough idea on the relative size one has to expect for the rare lepton decays $l_i \to l_j \gamma$

$$Br(l_i \to l_j \gamma) \propto \alpha^3 m^5_{l_i} \frac{|m^2_{L,ij}|^2}{\widetilde{m}^8} \tan^2 \beta$$

where $\widetilde{m}$ is the average of the SUSY masses involved in the loops.

- Note, that for a given set of high scale parameters both, the different size of the flavour mixing entries and the changed mass spectrum, play a role.

The Numerical Procedure

- All the plots shown below are based on the program packages `SPheno` and `micrOMEGAs`.
- We use `SPheno` version 3, including the RGEs for Seesaw Type I, II and III at the 2-loop level (calculated with `Sarah`).
- For any given set of mSugra and type-I, type-II or type-III parameters, SPheno calculates the supersymmetric particle spectrum at the electro-weak scale, which is then interfaced with micrOMEGAs2.4 to calculate the relic density of the lightest neutralino, $\Omega_{\chi_1^0} h^2$. All points satisfy neutrino data.
- For the standard model parameters we use the PDG 2008 values. As discussed below, especially important are the values (and errors) of the bottom and top quark masses, $m_b = 4.2 + 0.17 - 0.07$ GeV and $m_t = 171.2 \pm 2.1$ GeV. Note, the m_t is understood to be the pole-mass and $m_b(m_b)$ is the $\overline{MS}$ mass.
- For the allowed range for $\Omega_{DM} h^2$ we always use the 3 σ c.l. boundaries, i.e. $\Omega_{DM} h^2 = [0.081, 0.12.69]$. Note, however that the use of 1 σ contours results in very similar plots, due to the small error bars.
- We define our "standard choice" of mSugra parameters as $\tan\beta = 10$, $A_0 = 0$ and $\mu > 0$ and use these values in all plots, unless specified otherwise.

Dark Matter: co-annihilation region

- As is well-known, within mSUGRA there are 4 regions in parameter space, in which the constraint from dark matter can be satisfied. These are (i) the bulk region; (ii) the stau co-annihilation region; (iii) the focus point line and (iv) the Higgs funnel.

- In particular, the co-annihilation region is very sensitive to the difference between the masses of the lightest stau and the lightest neutralino. For a fixed $M_{1/2}$ and m_0 lowering the seesaw scale increases this mass difference, which then leads to a larger calculated Ωh^2. To compensate for this effect one needs to lower m_0, with the value depending on the seesaw scale chosen. For certain seesaw scales then m_0 needs to be lowered below $m_0 = 0$ and the co-annihilation region disappears.

Dark Matter: co-annihilation region

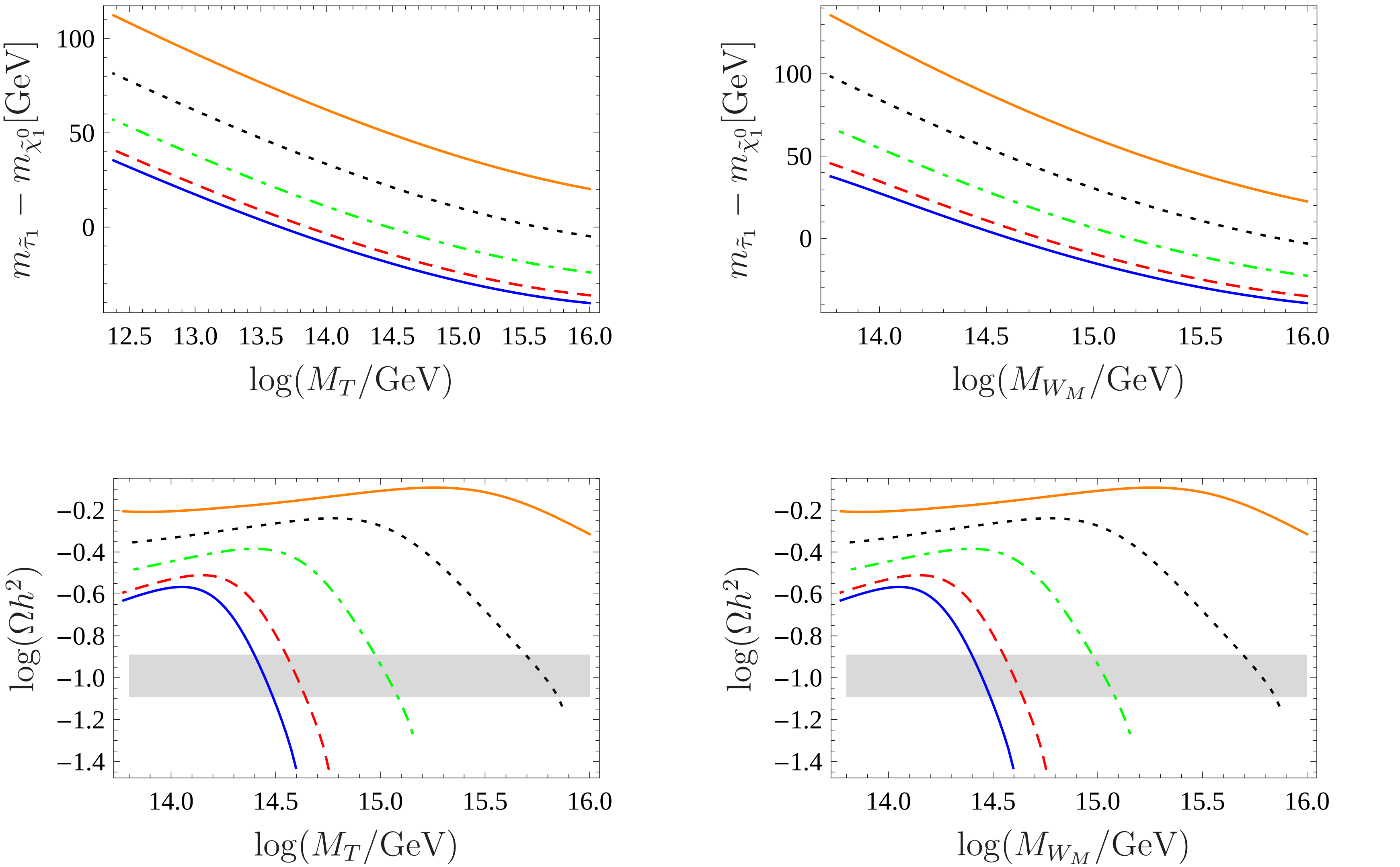

The left (right) plots are for seesaw type-II (III). $M_{1/2} = 800$ GeV, $A_0 = 0$, $\tan\beta = 10$ and $\mu > 0$. Color codes: full blue line $m_0 = 0$, red dashed line $m_0 = 50$ GeV, green dashed dotted line $m_0 = 100$ GeV, black dashed line $m_0 = 150$ GeV and orange full line $m_0 = 200$ GeV. The gray band shows the preferred $\Omega_{DM} h^2$ range.

Dark Matter: focus point

- The focus point region is very sensitive to the precise values of the input parameters. The focus point region appears in mSUGRA for large values of m_0 and small/moderate values of $M_{1/2}$ of the order of $\mathcal{O}(100)$ GeV, the exact value depending on m_0.
- We find that type-II and type-III behave differently in this region of parameter space, e.g. the higgsino content $|N_{13}|^2 + |N_{14}|^2$ decreases (increases) with increasing values m_0 for seesaw type-II (type-III).
- The increased higgsino content of the lightest neutralino leads to on increase (decrease) of its couplings to the Z-boson and the light Higgs boson (to sfermions) resulting in the observed dependence of Ωh^2.

Dark Matter: focus point

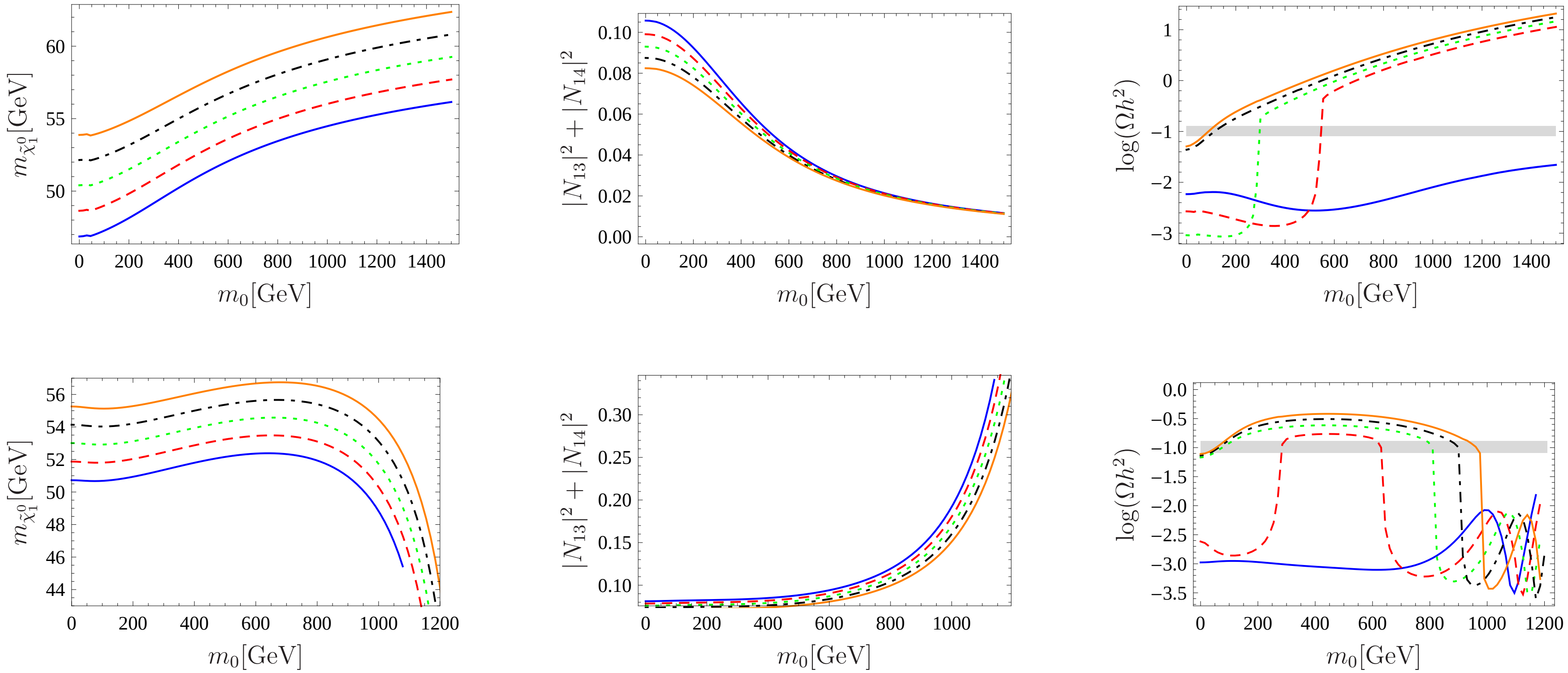

Mass of the lightest neutralino (left plot), its higgsino content (middle plot) and the corresponding Ωh^2 (right plot) as a function of m_0 for a seesaw type-II (top) and type-III (bottom) with $M_{\text{Seesaw}} = 10^{14}$ GeV, $m_{top} = 171.2$ GeV, $A_0 = 0$, $\tan\beta = 10$ and $\mu > 0$. Type-II: full blue line $M_{1/2} = 195$ GeV, red dashed line $M_{1/2} = 200$ GeV, green dashed dotted line $M_{1/2} = 205$ GeV, black dashed line $M_{1/2} = 210$ GeV and orange full line $M_{1/2} = 215$ GeV. Type-III: full blue line $M_{1/2} = 400$ GeV, red dashed line $M_{1/2} = 405$ GeV, green dashed dotted line $M_{1/2} = 410$ GeV, black dashed line $M_{1/2} = 415$ GeV and orange full line $M_{1/2} = 420$ GeV. The gray band shows the preferred Ωh^2 range.

Dark Matter Contours: mSugra & type-I

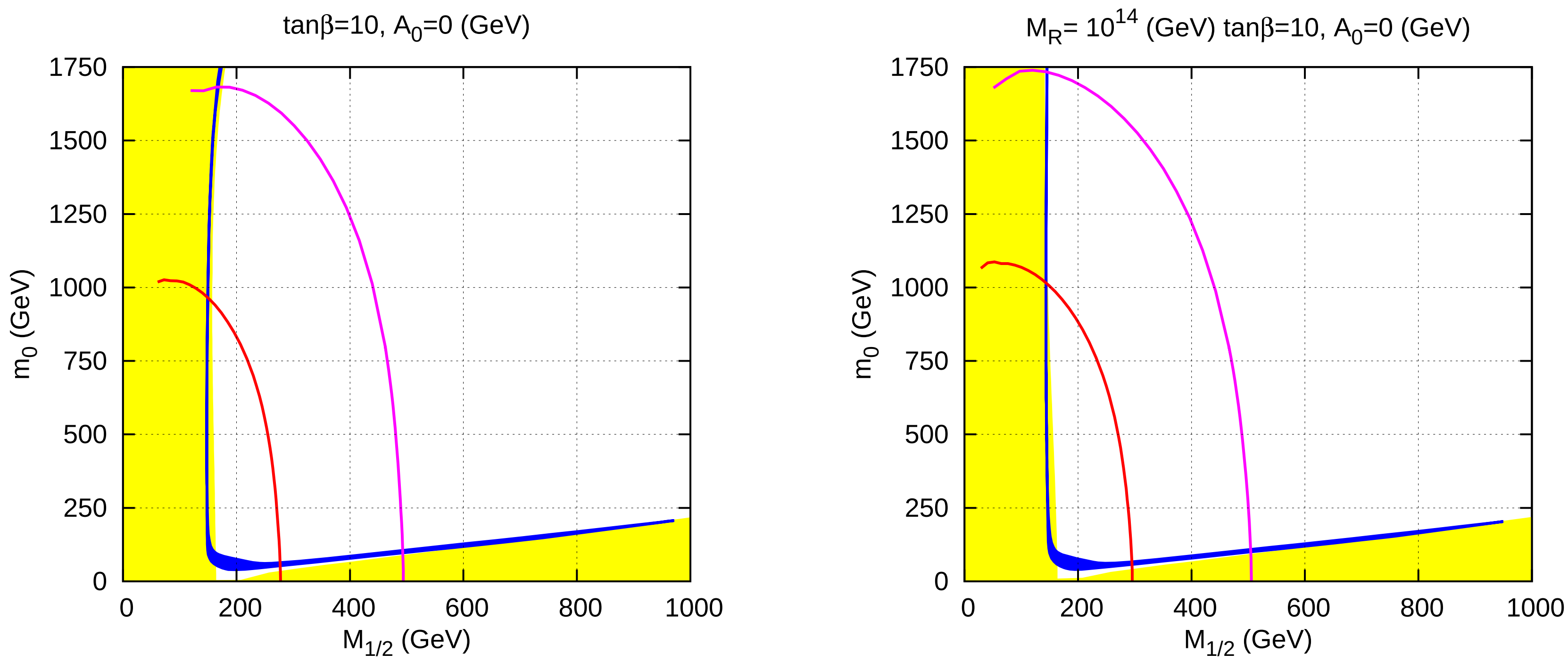

Dark matter allowed region (in blue) for mSUGRA (left panel) and for type-I seesaw (right panel). The parameters are $\tan\beta = 10$, $A_0 = 0$, $\mu > 0$ and $M_T = 10^{14}$ GeV for $m_{top} = 171.2$ GeV. Also shown (in yellow) are the regions excluded by LEP (small values of $M_{1/2}$), and by LSP constraint (small values of m_0). Also shown are the Higgs boson mass curves for $M_h = 110$ GeV (in red) and for $M_h = 114.4$ GeV (in magenta).

Dark Matter Contours: type-II & type-III

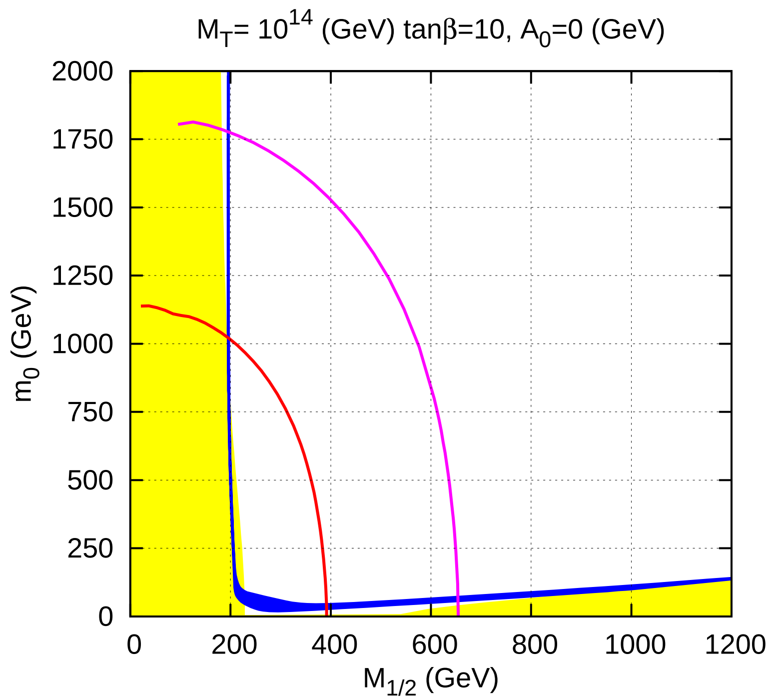

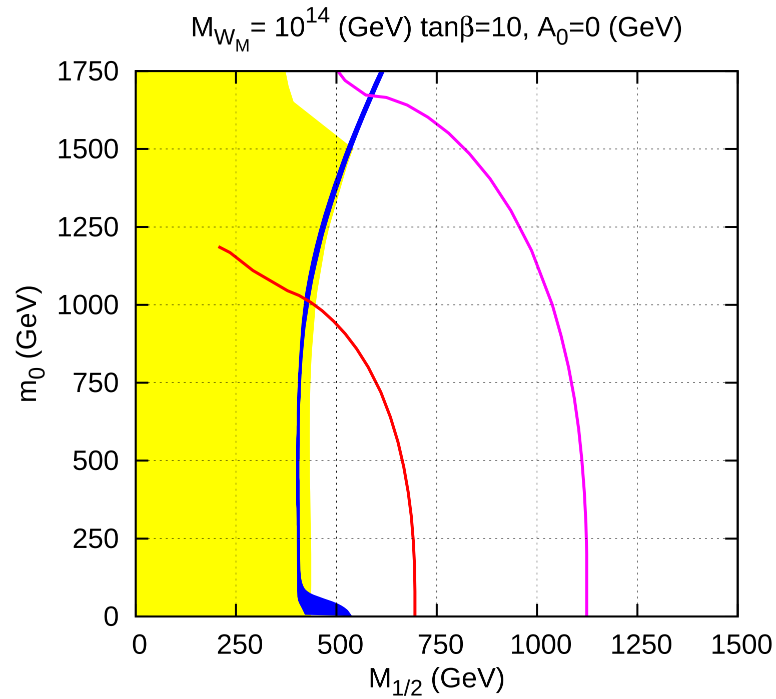

As before for seesaw type-II (left panel) and type-III (right panel).

Dark Matter Contours: type-II & type-III

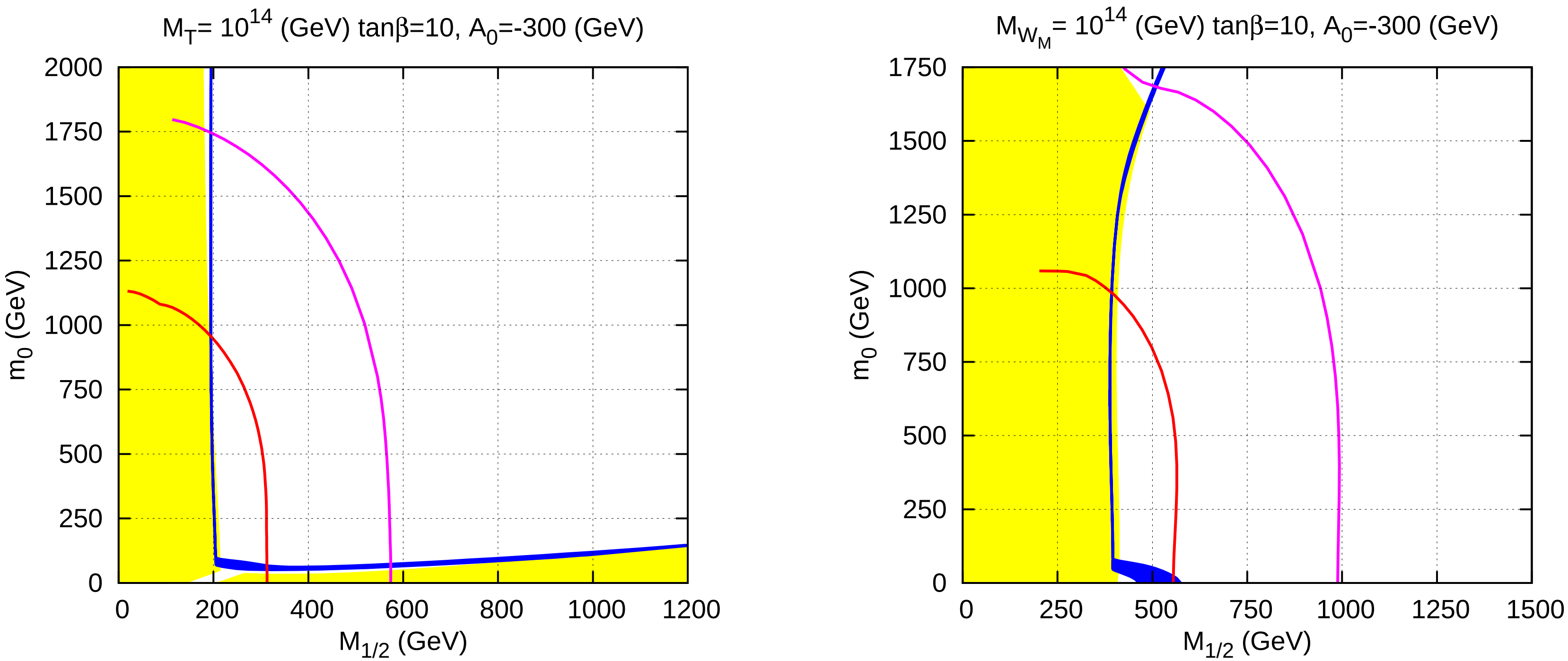

As before but for $A_0 = -300$ GeV. Seesaw type-II (left panel) and type-III (right panel).

Dark Matter Contours: Higgs Funnel

- In the case of large $\tan\beta$ an additional region, usually called the Higgs funnel, opens up. This region is characterized by $M_A \simeq 2m_{\tilde{\chi}_1^0}$.
- Also here the regions gets shifted compared to usual mSUGRA scenario. However, this region is very sensitive to higher order corrections and therefore it is quite important to use full 2-loop RGEs.
- The main reason for the observed and rather surprisingly large differences between the different calculations is that the 2-loop contributions decrease the neutralino mass compared to the 1-loop case while at the same time increasing M_A. For example, in case of seesaw II and for fixed values of $m_0 = M_{1/2} =$ 1500 GeV we get in case of 1-loop RGEs $m_{\tilde{\chi}_1^0} = 560$ GeV, $M_A = 1090$ GeV and in case of 2-loop RGEs $m_{\tilde{\chi}_1^0} = 498$ GeV, $M_A = 1100$ GeV.

Dark Matter Contours: Higgs Funnel (1-loop vs 2-loop)

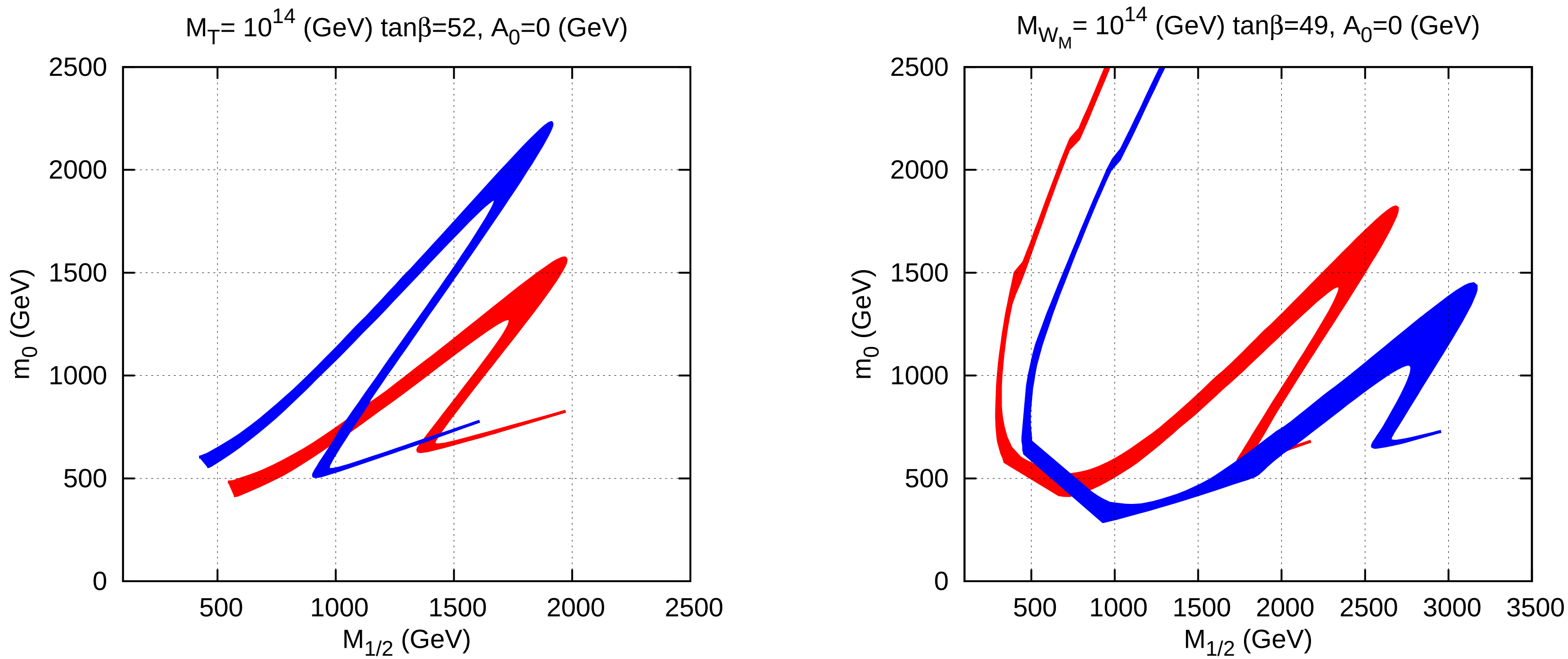

Comparison between using 1-loop (red) or 2-loop (blue) RGEs on the dark matter allowed region for type-II (left panel) and type-III (right panel). The parameters are: $A_0 = 0$, $\mu > 0$ and $M_{\rm Seesaw} = 10^{14}$ GeV, $m_{top} = 171.2$ GeV and $\tan\beta = 52$ for type-II and $\tan\beta = 49$ for type-III.

Variation with the Seesaw Scale

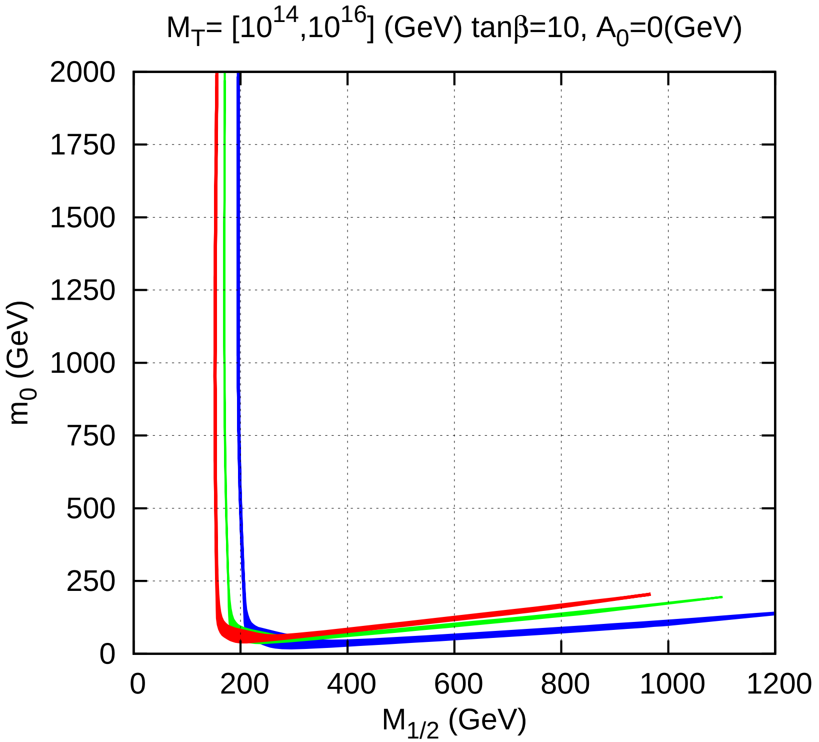

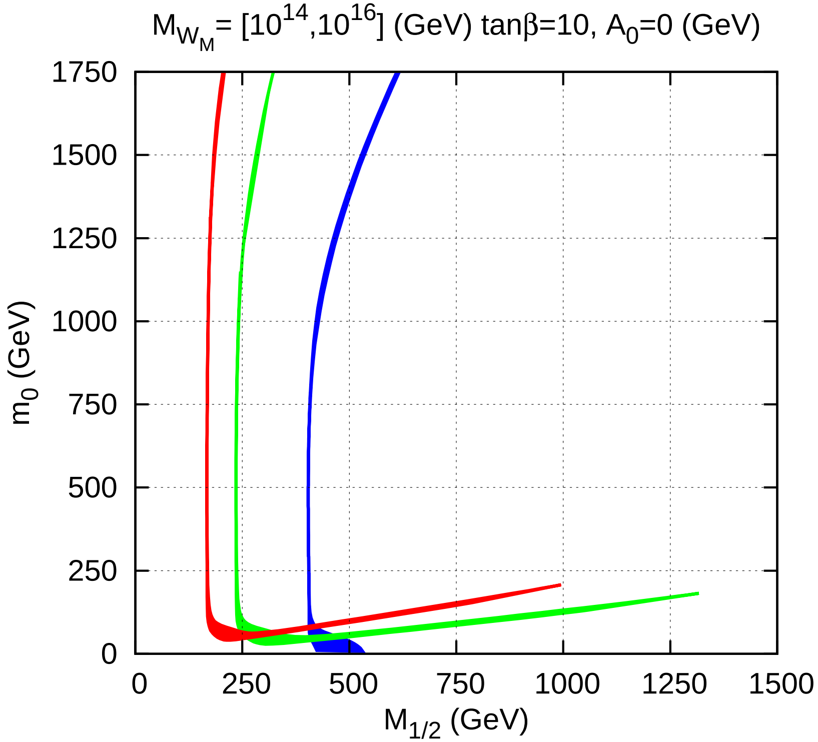

Allowed region for dark matter density $(0.081 < \Omega_{\chi_1^0} h^2 < 0.129)$ in the $(m_0, M_{1/2})$ plane for the "standard choice" $\tan\beta = 10$, $A_0 = 0$ and $\mu \geq 0$, for three values from M_T, $M_T = 10^{14}$ GeV (blue), to $M_T = 10^{16}$ GeV (red). Left (right) for panel type-II (type-III).

Variation of the Higgs Funnel with M_{Seesaw}

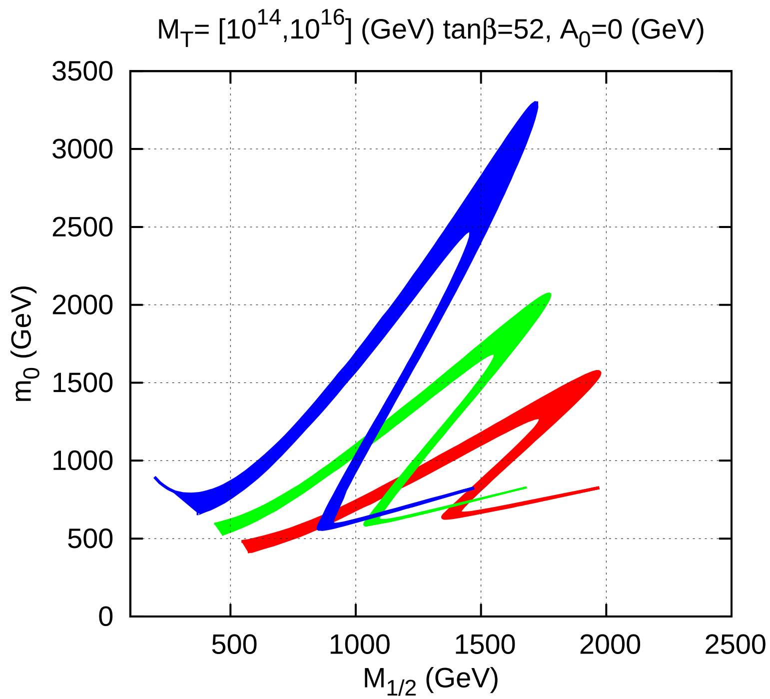

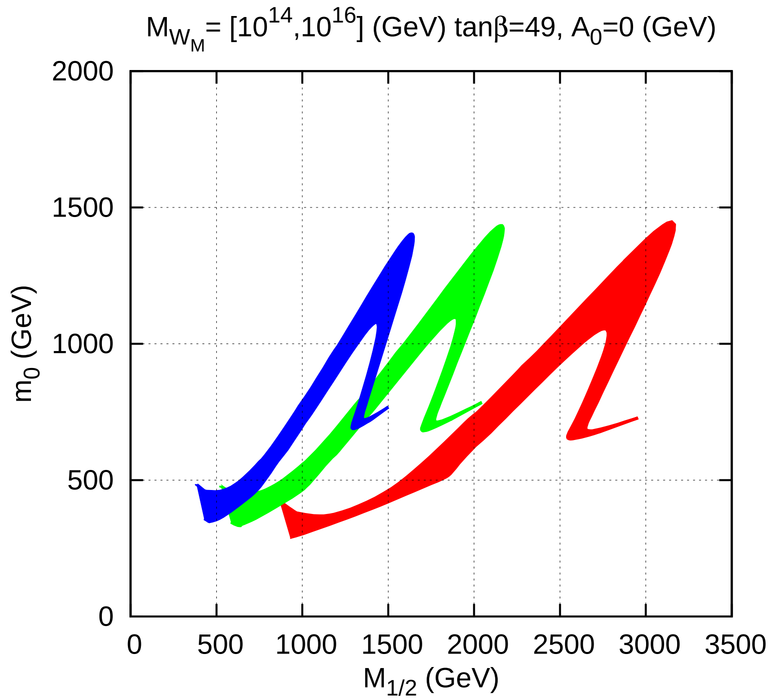

Allowed region for dark matter density in the $(m_0, M_{1/2})$ plane for $A_0 = 0$, $\mu \geq 0$, for (from bottom to top) $M_T = 10^{14}$ GeV (red), $M_T = 10^{15}$(green) and $M_T = 10^{16}$ GeV (blue). Left panel for seesaw type-II with $\tan\beta = 52$ and right panel for seesaw type-III with $\tan\beta = 49$.

Variation of the Higgs Funnel with m_{top} & m_b (type-II)

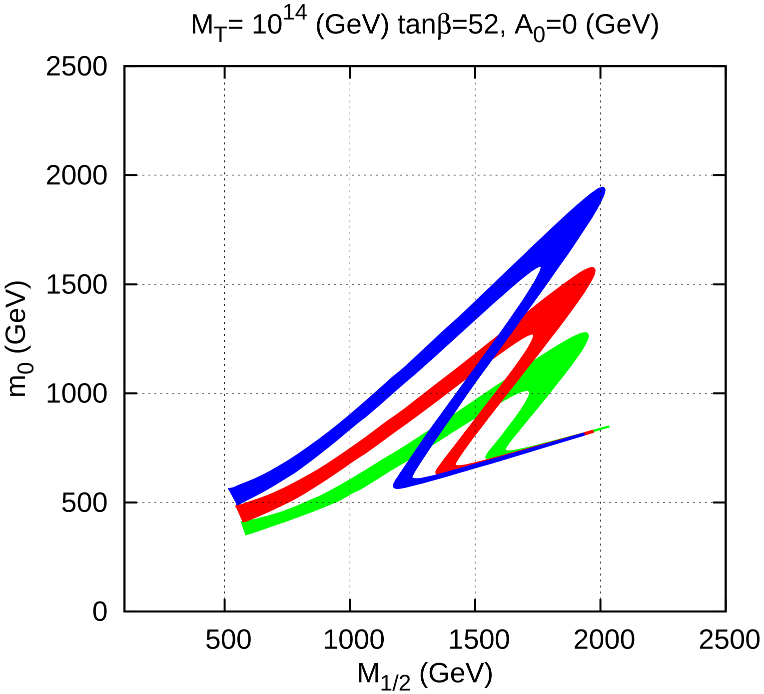

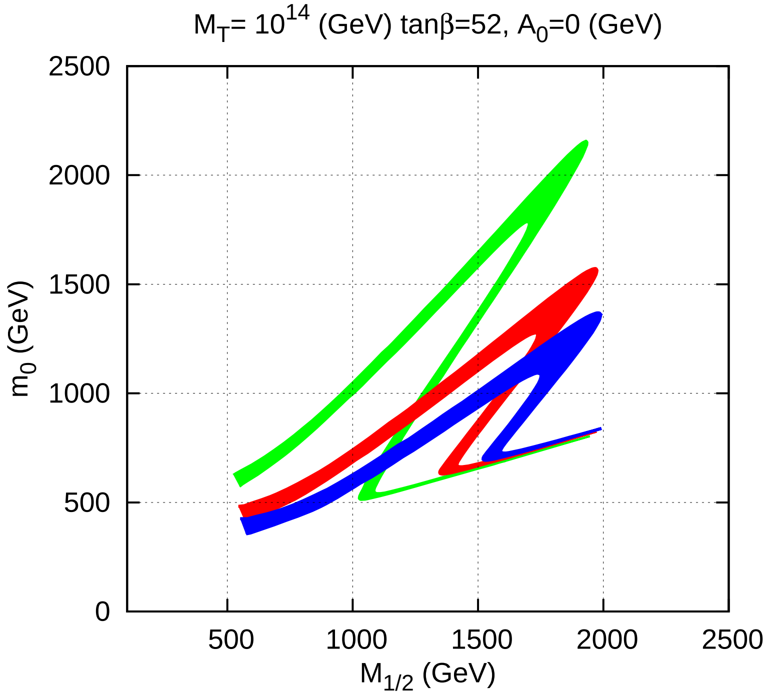

Allowed region for the dark matter density in the $(m_0, M_{1/2})$ plane for $A_0 = 0$, $\mu \geq 0$ and $\tan\beta = 52$, for $M_T = 10^{14}$ GeV and (to the left) for three values of $m_{top} = 169.1$GeV (blue), $m_{top} = 171.2$ GeV (red) and $m_{top} = 173.3$ GeV (green). To the right: The same, but varying m_b. $m_{bot} = 4.13$ GeV (blue), $m_{bot} = 4.2$ GeV (red) and $m_{bot} = 4.37$ GeV (green).

Variation of the Higgs Funnel with $m_{\rm top}$ & m_b (type-III)

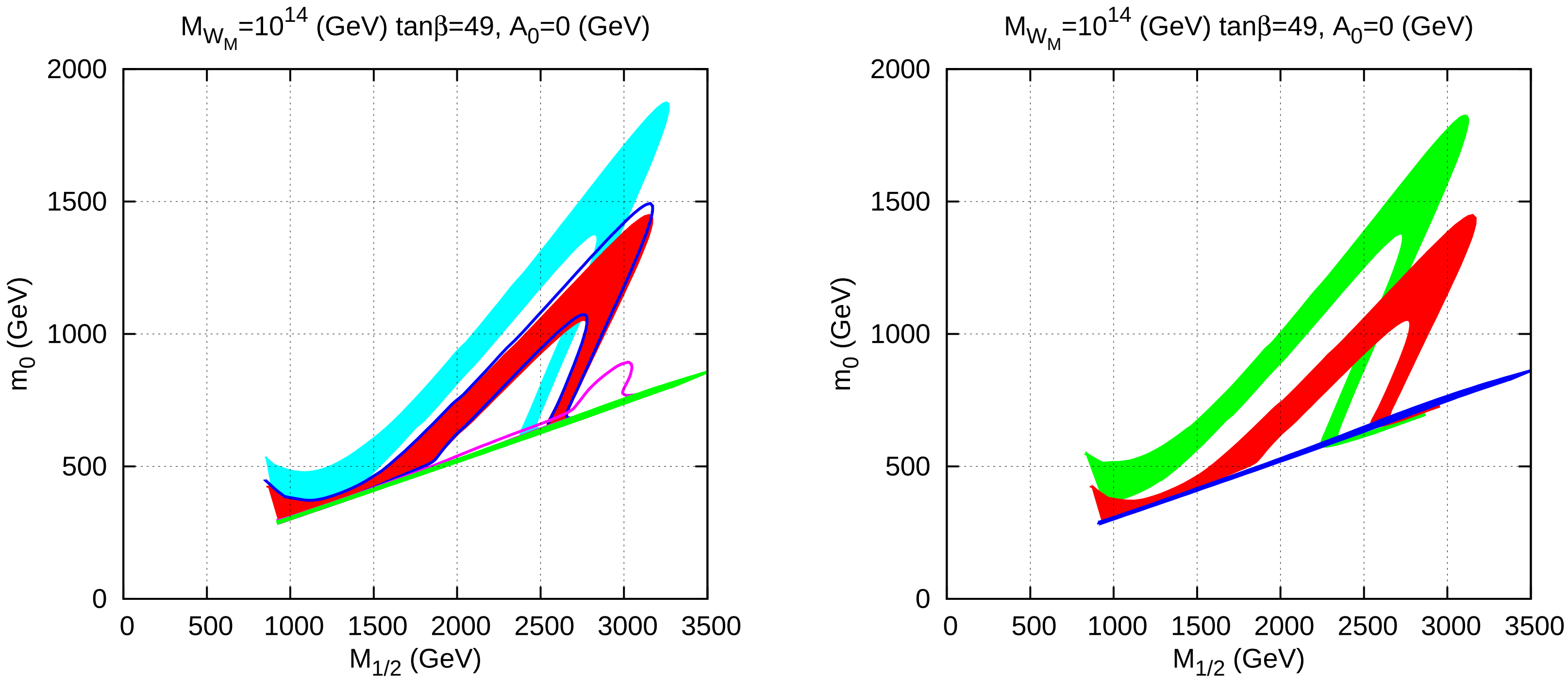

Allowed region for the dark matter density in the $(m_0, M_{1/2})$ plane for $A_0 = 0$, $\mu \geq 0$ and $\tan\beta = 52$, for $M_T = 10^{14}$ GeV and (to the left) for five values of $m_{top} = 168$GeV (cyan) $m_{top} = 169.1$GeV (blue), $m_{top} = 171.2$ GeV (red), $m_{top} = 171.4$ GeV (magenta) and $m_{top} = 173.3$ GeV (green). To the right: The same, but varying m_b. $m_{bot} = 4.13$ GeV (blue), $m_{bot} = 4.2$ GeV (red) and $m_{bot} = 4.37$ GeV (green).

Lepton flavour violation

- The rates for LFV decays of μ and τ scale like the LFV entries in the slepton mass squared matrix squared and inverse to the overall SUSY mass to the power eight.
- From this one immediately concludes the rates for the rare lepton decays are in general larger in seesaw models of type-II and III than in type-I models for fixed SUSY masses and seesaw scales except if one arranges for special cancellations.
- Comparing the type-II with the type-III model one finds that LFV decays are larger for type-III. Naively, one would expect that type-II should have larger LFV. Numerically we find the opposite for two reasons. (i) $Br(l_i \to l_j\gamma)$ strongly depends on the SUSY masses, and type-III has a lighter spectrum than type-II (for the same mSUGRA input parameters). And (ii) 2-loop effects are very important in type-III, due to the large coefficients, in general leading to large flavor violating soft SUSY breaking parameters.

Comparison of $\mu \to e\gamma$ for the three sessaw types

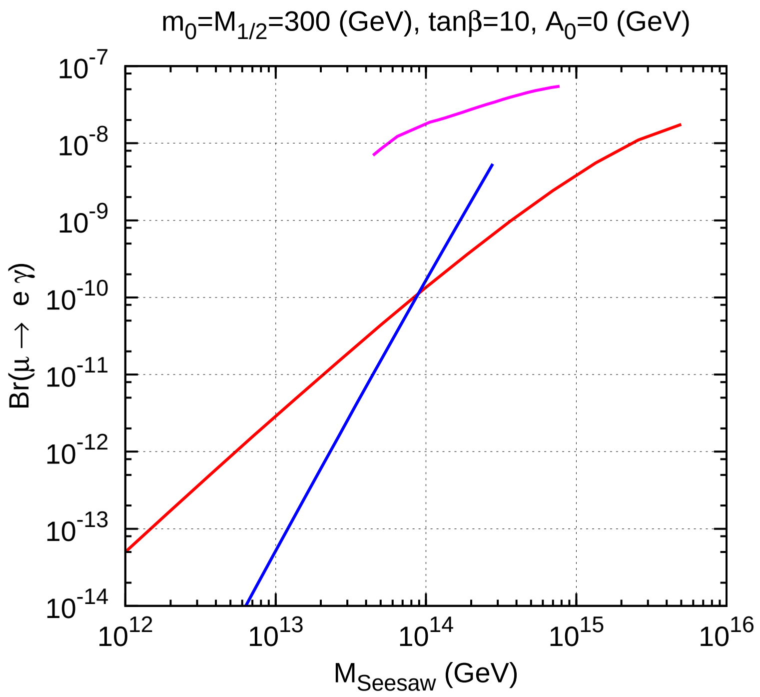

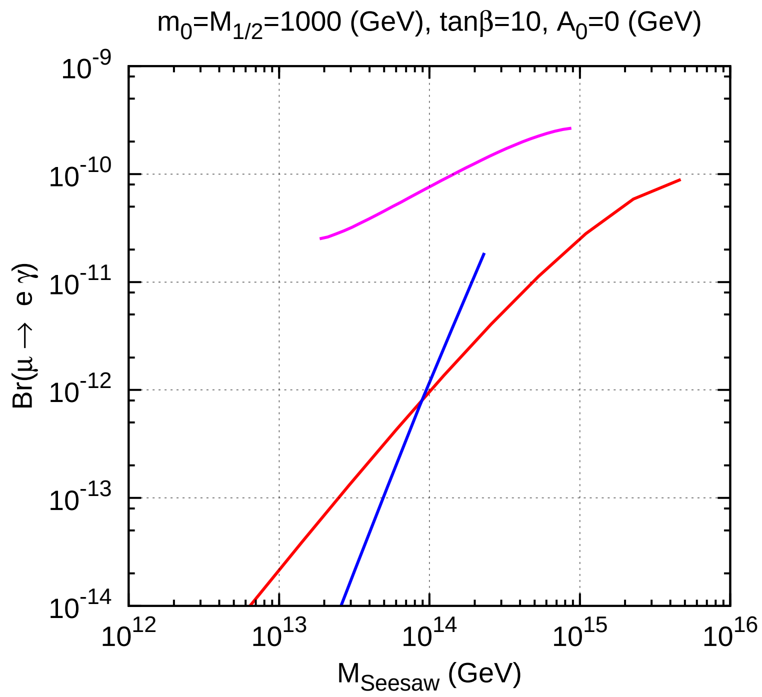

$Br(\mu \to e\gamma)$ as a function of the seesaw scale for seesaw type-I (red line), seesaw type-II (blue line) and seesaw type-III (magenta line). In case of type-I and type-III a degenerate spectrum has been assumed. On the left panel $m_0 = m_{1/2} = 300$ (GeV), on the right panel $m_0 = m_{1/2} = 1000$ (GeV). In both cases we take $\tan\beta = 10$, A_0=0 and $\mu > 0$.

Possible way out for type-III: Cancellations

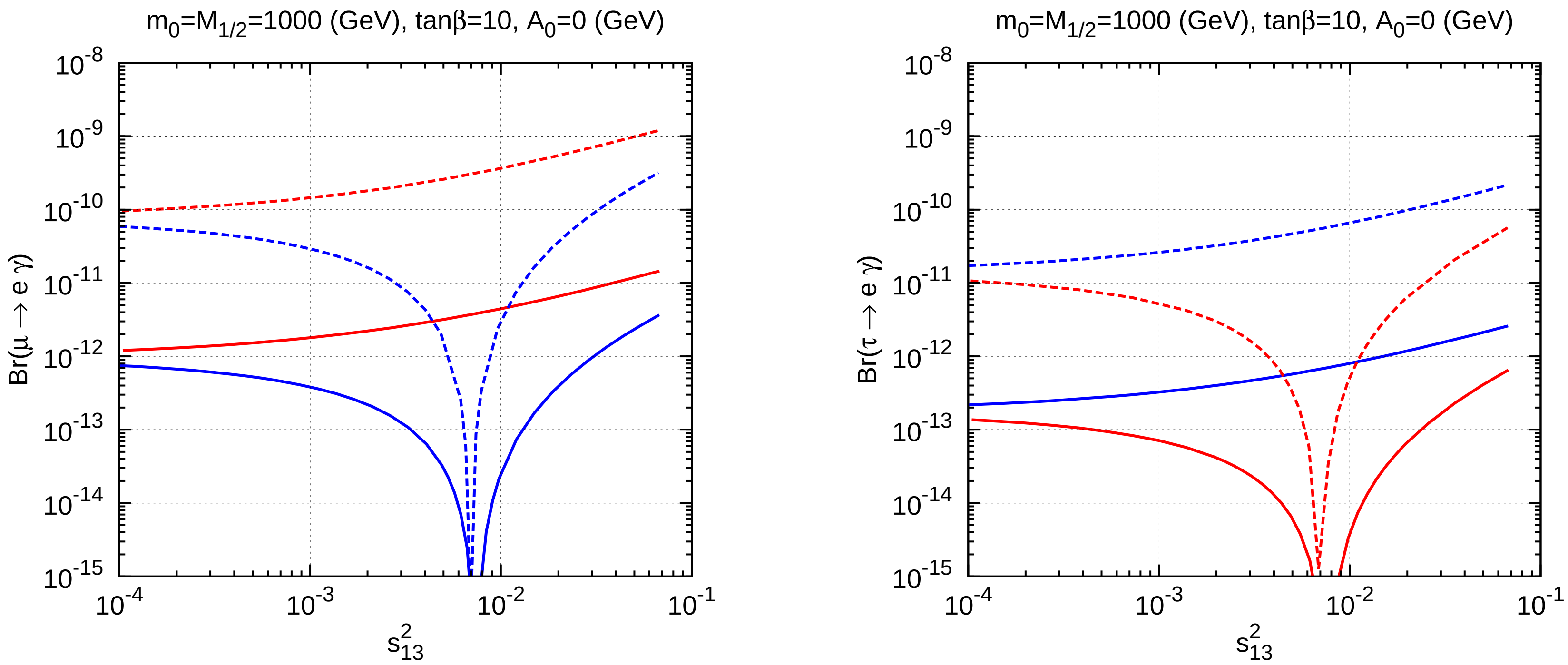

$Br(\mu \to e\gamma)$ (left) and $Br(\tau \to e\gamma)$ (right) versus s_{13}^2 for $m_0 = M_{1/2} = 1000$ GeV, $\tan\beta = 10$, $A_0 = 0$ GeV and $\mu > 0$, for seesaw type-I (solid lines) and seesaw type-III (dashed lines), for $M_{\rm Seesaw} = 10^{14}$ GeV. The curves shown are for 2 values of the Dirac phase: $\delta = 0$ (red) and $\delta = \pi$ (blue), both for normal hierarchy.

Possible way out for type-III: Cancellations

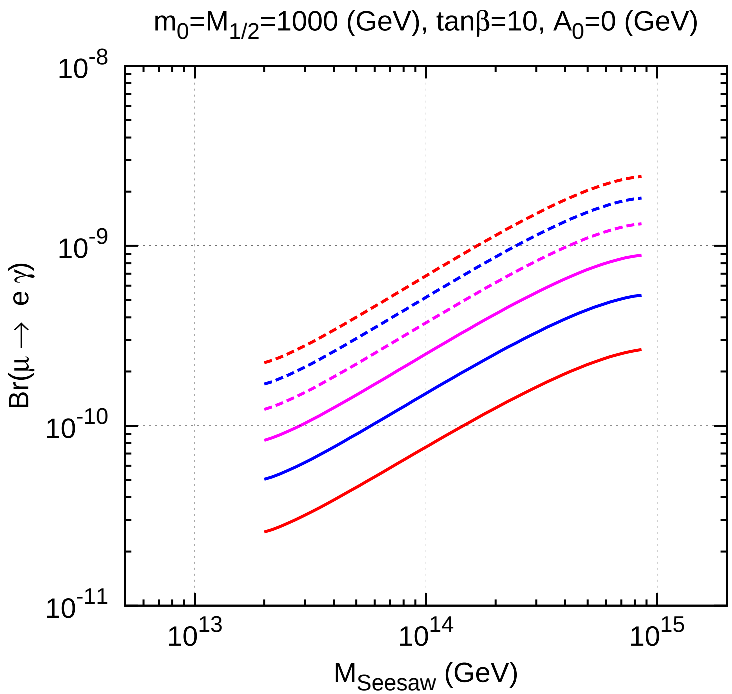

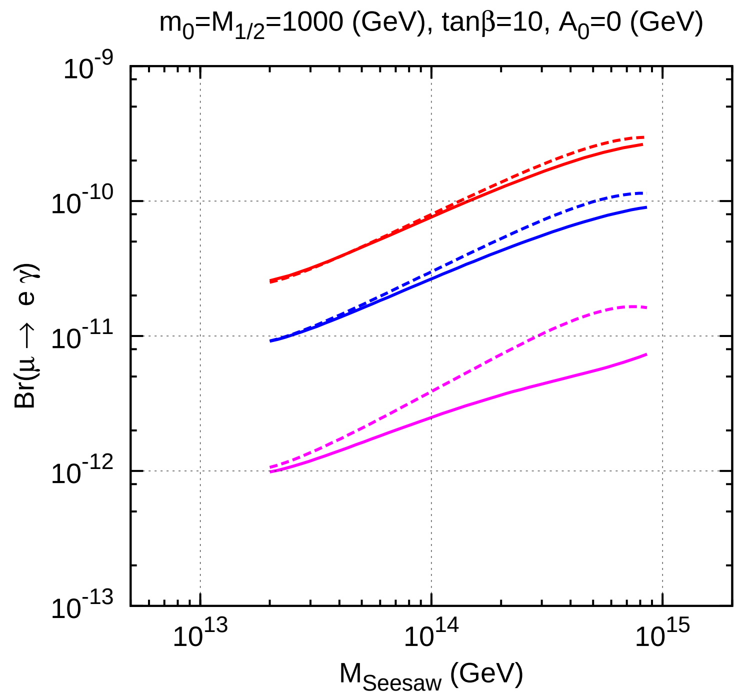

$\mu \to e\gamma$ versus M_{SS} for $m_0 = M_{1/2} = 1000$ GeV, $\tan\beta = 10$, $A_0 = 0$ GeV and $\mu > 0$, for seesaw type-III. On the left $\delta_{\rm Dirac} = 0$ and on the right $\delta_{\rm Dirac} = \pi$. The curves shown are for $\theta_{13} = 0$ (solid red), $\theta_{13} = 2$ (solid blue), $\theta_{13} = 4$ (solid magenta), $\theta_{13} = 6$ (dashed magenta), $\theta_{13} = 8$ (dashed blue), $\theta_{13} = 10$ (dashed red).

Cancellations: Comments

- At first glance this seem to require some fine-tuning of the underlying parameters.
- However, one can look at this from a different perspective: Assume that the MEG collaboration has found a non-vanishing value for $Br(\mu \to e\gamma)$ and from LHC data one has found that the spectrum is consistent with the type-III seesaw model. For a fixed R-matrix, e.g. $R=\mathbf{1}$ one would obtain in this case a relation between s^2_{13} and M_{24}.
- This can be exploited to put a bound on M_{24} or even to determine it depending on the outcome of measurements of reactor angle and, thus, the model assumptions can be tested.

The effect of non-degenerate spectra

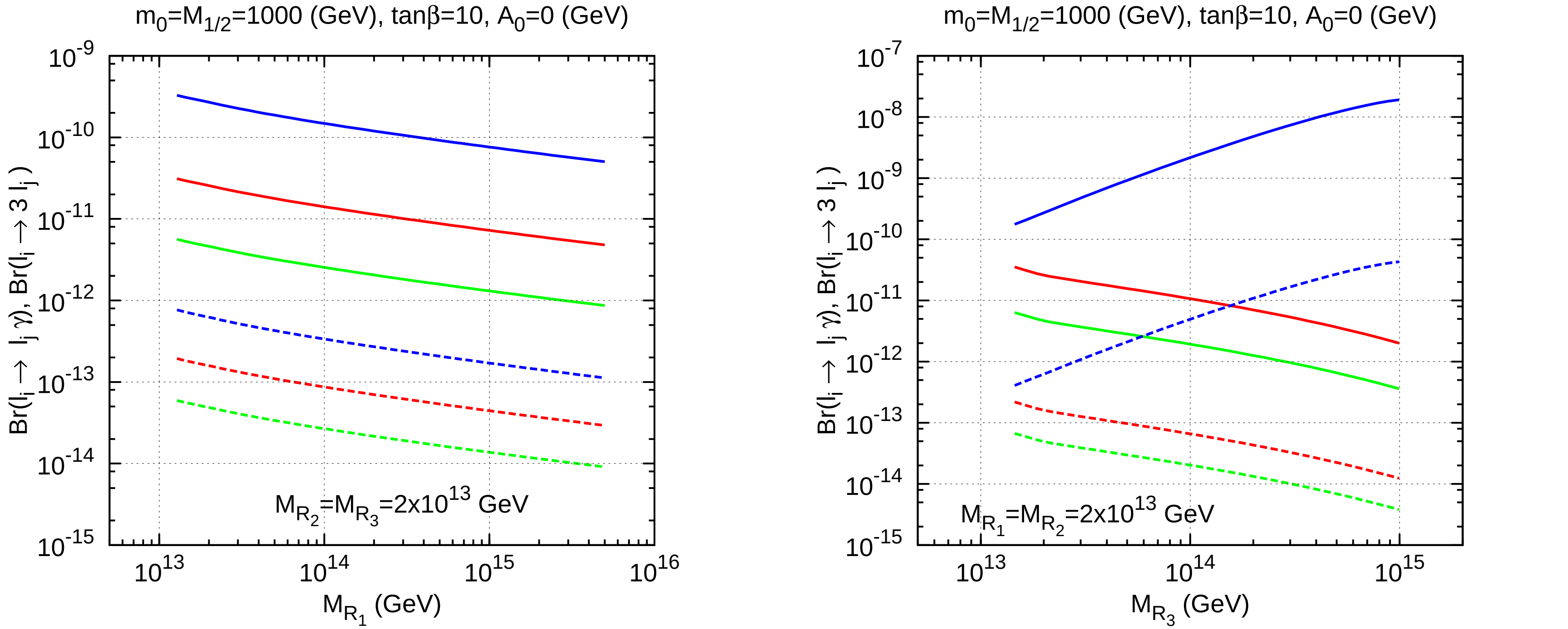

Branching ratios for $l_i \to l_j\gamma$ (solid lines) and $l_i \to 3l_j$ (dashed lines) versus the seesaw scale for $\tan\beta = 10$, $\mu > 0$, $A_O = 0$ GeV, $M_{1/2} = m_0 = 1000$ GeV. On the left panel we scan on M_{R_1} with $M_{R_2} = M_{R_3} = 2 \times 10^{13}$ GeV while on the right panel we scan on M_{R_3} with $M_{R_1} = M_{R_2} = 2 \times 10^{13}$ GeV. The color code is red for $\mu \to e\gamma$ or $\mu \to 3e$, blue for $\tau \to \mu\gamma$ or $\tau \to 3\mu$ and green for $\tau \to e\gamma$ or $\tau \to 3e$.

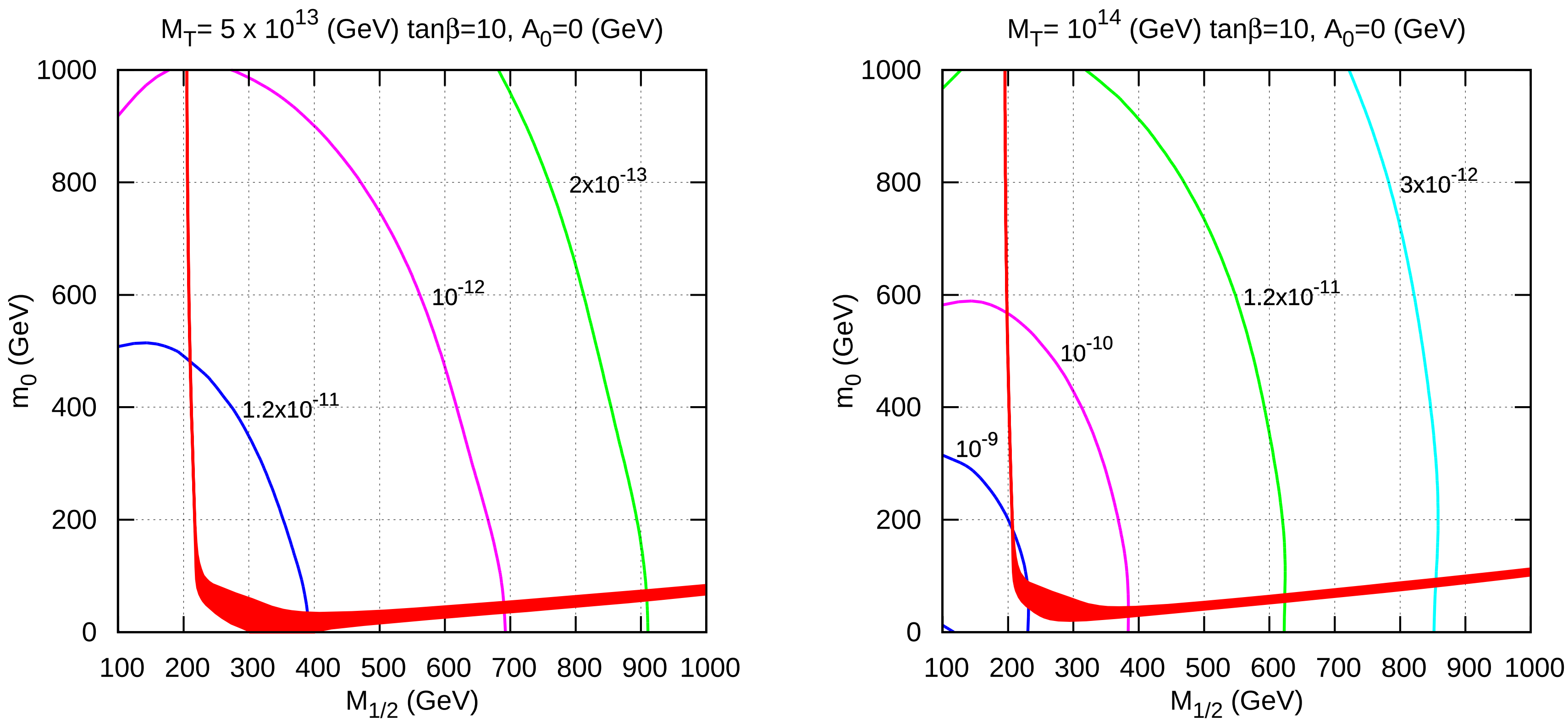

Allowed region for dark matter density in the $(m_0, M_{1/2})$ plane for type-II and for our "standard choice" of mSugra parameters and for two values of M_T: $M_T = 5 \times 10^{13}$ (left panel) and for $M_T = 10^{14}$ (right panel). Superimposed are the contour lines for the $Br(\mu \to e\gamma)$.

DM & LFV: Seesaw type-I

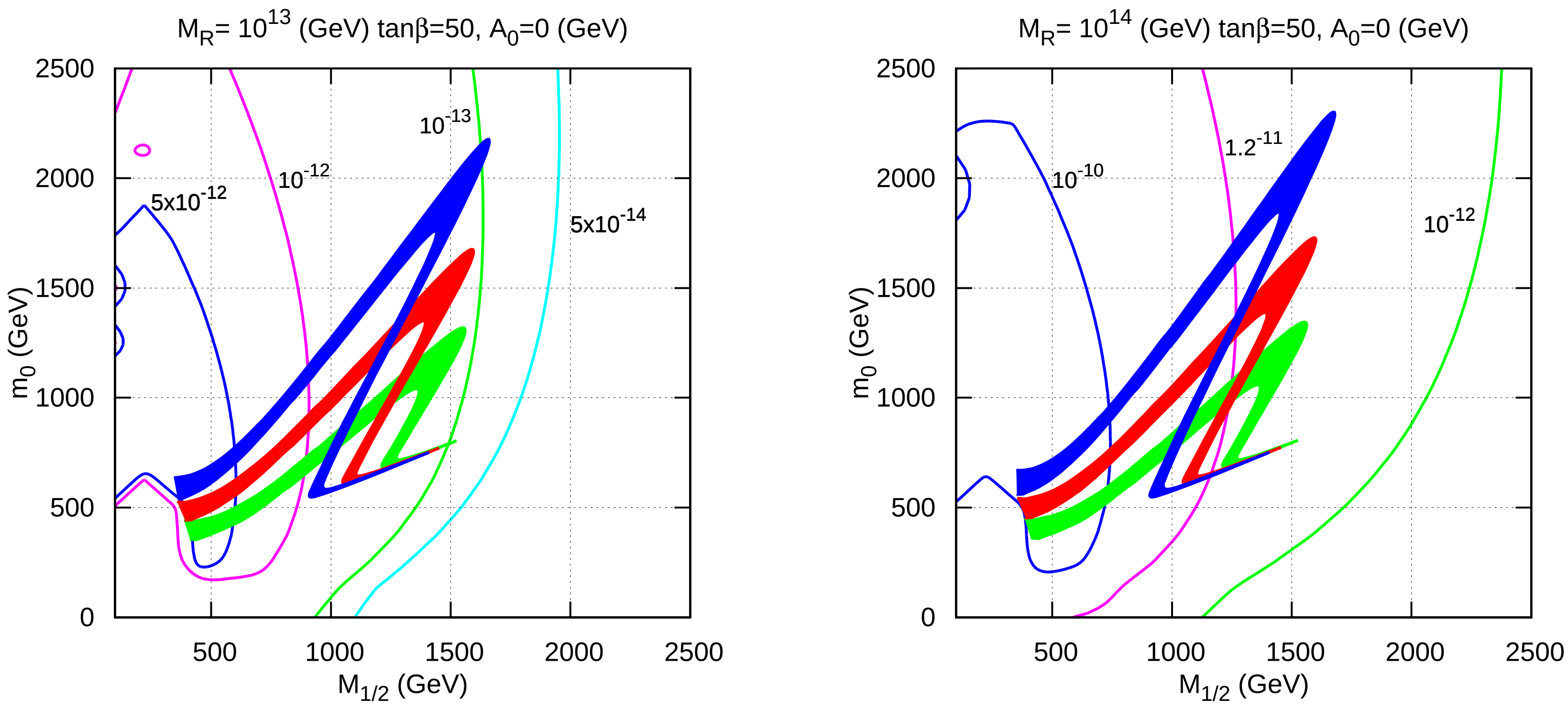

Allowed region for dark matter density $(0.081 < \Omega_{\chi_1^0} h^2 < 0.129)$ in the $(m_0, M_{1/2})$ plane for $A_0 = 0$, $\mu \geq 0$ and $\tan\beta = 52$, for three values of $m_{top} = 169.1$ GeV (blue), $m_{top} = 171.2$ GeV (red) and $m_{top} = 173.3$ GeV (green) for $M_R = 10^{13}$ (left panel) and for $M_R = 10^{14}$ (right panel). Superimposed are the contour lines for the $Br(\mu \to e\gamma)$.

DM & LFV: Seesaw type-II

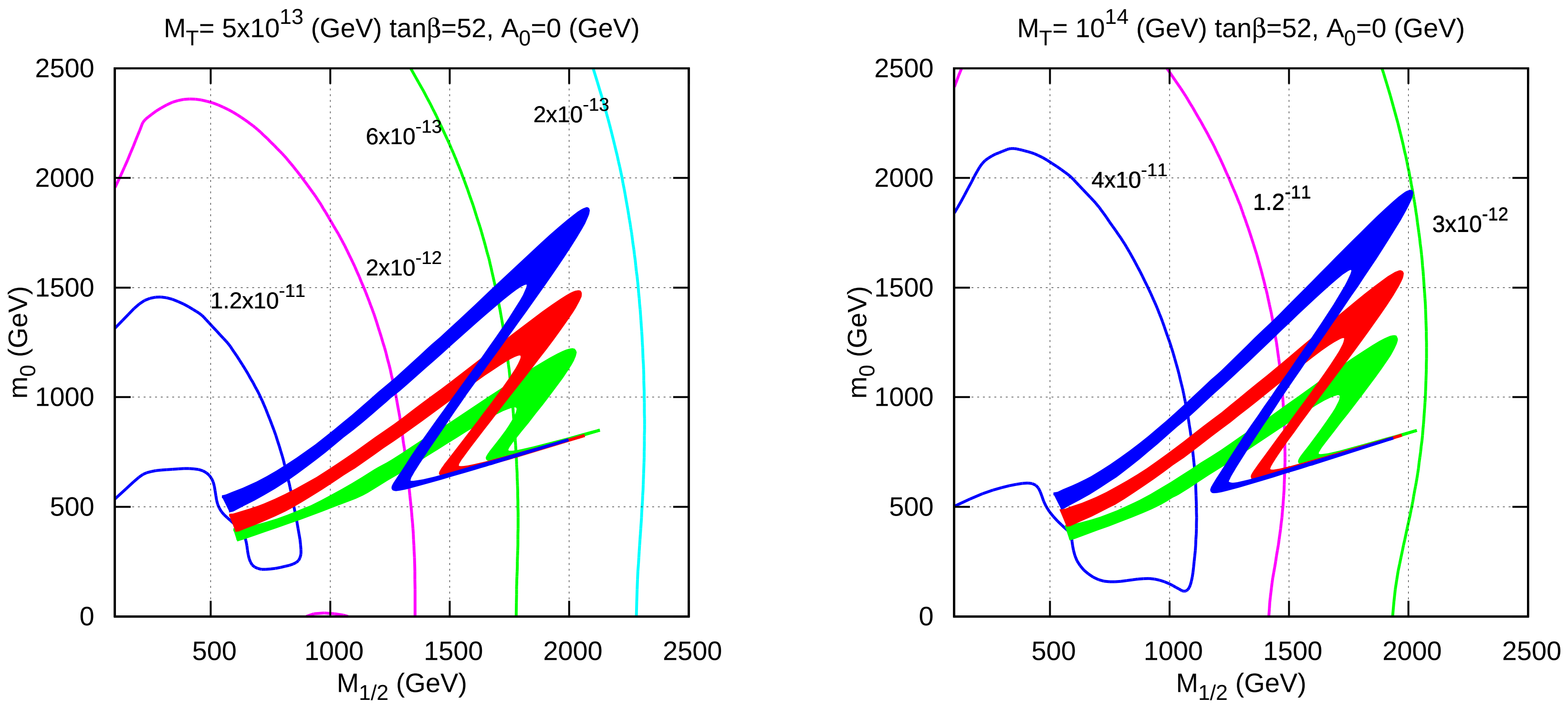

Allowed region for dark matter density $(0.081 < \Omega_{\chi_1^0} h^2 < 0.129)$ in the $(m_0, M_{1/2})$ plane for $A_0 = 0$, $\mu \geq 0$ and $\tan\beta = 52$, for three values of $m_{top} = 169.1$ GeV (blue), $m_{top} = 171.2$ GeV (red) and $m_{top} = 173.3$ GeV (green) for $M_T = 5 \times 10^{13}$ (left panel) and for $M_T = 10^{14}$ (right panel). Superimposed are the contour lines for the $Br(\mu \to e\gamma)$.

DM & LFV: Seesaw type-III

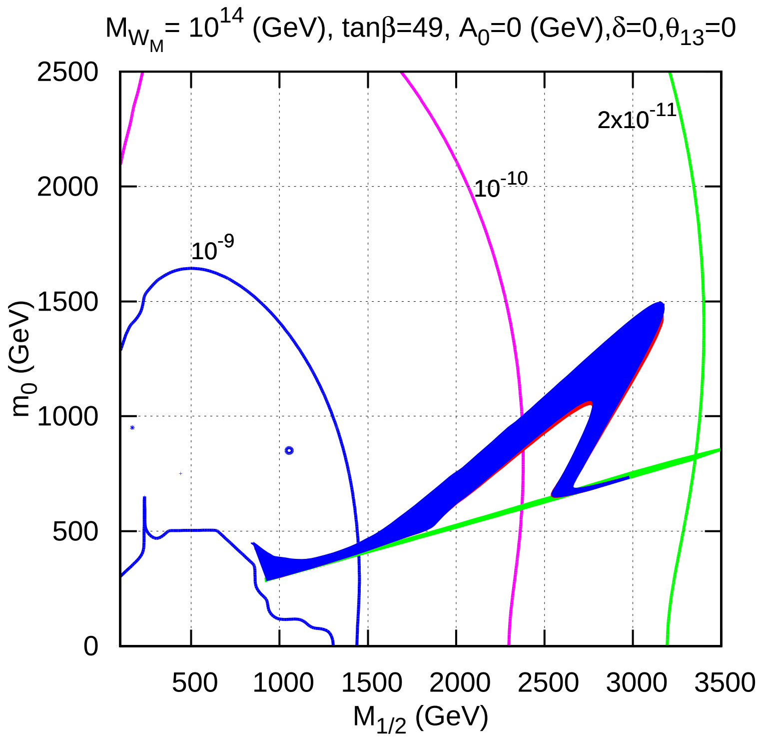

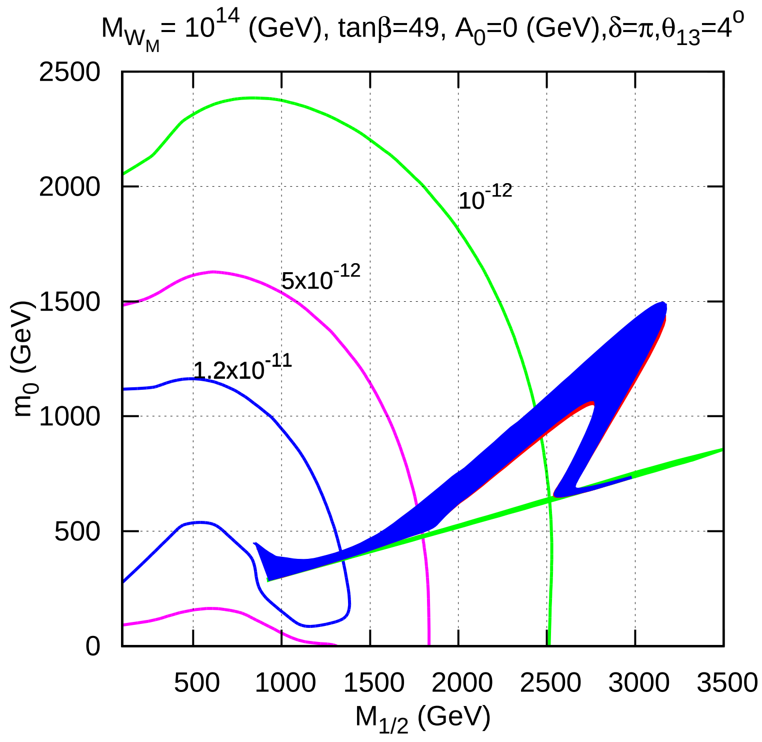

Allowed region for dark matter density ($0.081 < \Omega_{\chi_1^0} h^2 < 0.129$) in the $(m_0, M_{1/2})$ plane for $A_0 = 0$, $\mu \geq 0$ and $\tan\beta = 49$, for three values of $m_{top} = 169.1$ GeV (blue), $m_{top} = 171.2$ GeV (red) and $m_{top} = 173.3$ GeV (green) for $M_{W_M} = 10^{14}$. Superimposed are the contour lines for the $Br(\mu \to e\gamma)$ with $\delta = 0$, $\theta_{13} = 0$ (felt panel) and $\delta = \pi$, $\theta_{13} = 4^\circ$ (right).

Conclusions

- We have investigated in detail a supersymmetric model with mSugra boundary conditions including type-I, type-II or type-III seesaw mechanisms. In case of type-II and type-III models we have embedded the $SU(2)$ triplets in the corresponding $SU(5)$ representations to maintain gauge coupling unification, e.g. **15**-plets (type-II) and **24**-plets (type-III).
- The additional heavy charged states lead to changes in the beta-functions and, thus, also in the running of the SUSY mass parameters. Certain "invariants" contain indirect information about the seesaw scale assuming the type of seesaw model. In certain parts of the parameter space, e.g. for low seesaw scales, one might even be able to exclude certain seesaw models by combining mass measurements at the LHC with the mSUGRA paradigm. Using 2-loop RGEs will be crucial to obtain reliable results.
- We have calculated LFV, such as $Br(l_i \to l_j + \gamma)$. For fixed (degenerate) seesaw scale these branching ratios are in general largest for type-III models followed by type-II and type-I. This is a consequence of the fact that for a given set of mSUGRA parameters the spectrum in type-III is lighter than for type-II models which is again lighter than in type-I.
- We also calculated the relic density Ωh^2 for the three models. We find the usual four regions in the mSUGRA parameter space but of course they are shifted due to the changes in the spectrum. It has been found that in particular in case of the Higgs-funnel the use of 2-loop RGEs is crucial to identify the correct allowed region. For low seesaw scales the co-annihilation region vanishes for both, the type-II and the type-III models.
- The DM calculation suffers from a number of uncertainties, even if we assume the soft masses to be perfectly known. The most important SM parameters turn out to be the bottom and the top quark mass.